Mohamed Khider University of Biskra
Faculty of exact sciences and natural and life sciences
Material sciences department

MASTER MEMORY

Domain of Matter Sciences
Field : **Physics**
Speciality : **Energetic Physics and Renewable Energies**

Réf. : Entrez la référence du document

Presented by:
ZERGUINE Nafissa

The :

Elaboration and Characterization of Undoped and Cu doped TiO_2 thin films by Sol-Gel (Dip-Coating)

Jury:

Pr.	**RAHMANE Saâd**	**Professor**	**University of Biskra**	**President**
Pr.	**CHALA Abdelouahed**	**Professor**	**University of Biskra**	**Reporter**
Pr.	**SIAD Chahinez**	**Professor**	**University of Biskra**	**Examiner**

Academic Year : 2020 - 2021

Dedication

I dedicate this humble work :

To my beloved mother who lighted my path

To my dear father

To my brothers and sisters

To all my family

To my friends Cirta and Asma

To my colleagues: Benkhetta Okbaand Msabel Mabrouk

To everyone who supported me

To all who taught me a letter during my educational career

To everyone who loves knowledge and seeks to acquire it

Acknowledgment

First of all , all the praise and thanks to Allah the Almighty who helps me and gave me the will to do this humble work.

Afterwards, I would like to express my deep gratitude to my master thesis supervisor Mr. CHALA Abdelouahad, Professor at the University of Biskra and the director of the thin films laboratory and its applications, for all the knowledge, guidance and helping that he shared with me during the writing of this thesis. Nothing can reward his generosity and support. May Allah give him both the greatest rewards in the world and the Day After.

Also I sincerely thank the professors participating in the jury for examining my work.

I thank without exception everyone who supported me to complete this thesis, especially my colleagues Benkhetta Okba and Msabel Mabrouk.

Last but not the least important, I owe more than thanks to my parents and my family , for their financial support and encouragement throughout my life. Without their support, it is impossible for me to finish my college and graduate education seamlessly.

Contents

Chapter II: *Sol-Gel deposition method and characterization techniques*

Chapter III: *Results and Discussion*

General Introduction

Transparent conductive oxides are considered to be an important research topic in many useful applications thanks to the combination of optical transparency in the visible region and electrical conductivity which is a physical property unique to TCOs. They are generally prepared with thin film technologies and widely used in opto-electronic devices. Among all of the TCOs, Titanium dioxide (TiO_2) is the most attractive semiconductor due to its remarkable physical properties such as chemical and thermal stability, non-toxicity, transparent for visible light with wide optical band gap and high refractive index in addition to its abundance and its cheap price, make the latter a desirable candidate for use in various applications, the most important of which are pigments, photocatalysis, photovoltaic and gas sensors.

The aim of this master memory is to study the influence of copper doping at different concentrations on the structural, morphological and optical properties of titanium dioxide thin films. For that we will carry out a series of samples on the glass substrates by the sol-gel dip coating method, and then we will anneal the samples at 400 °C for 3 hours, for better crystallinity.

The study is divided into three chapters which are organized as follows:

The first chapter concerns a bibliographical study about transparent conductive oxides (TCO), their physical properties and applications, then we will allocate of which the titanium dioxide, its physical properties (structural, optical and electrical) and some applications of this oxide. In addition to the doping of TiO_2 and the different deposition methods to synthesize Cu doped TiO_2 thin films.

The second chapter is devoted to a definition of sol-gel deposition method and then the followed experimental procedure to deposit pure TiO_2 and Cu doped TiO_2 thin films by means sol-gel dip coating deposition method, as well as the methods of structural, morphological and optical characterizations used in this work.

The third chapter deals with the discussion and analysis of the obtained results in this study.

Finally, the memory ends with a general conclusion.

Chapter 1

Bibliographical Study

In this chapter we will present a bibliographical study about transparent conductive oxides (TCO) , their physical properties and applications in a general and brief manner , and specifically we will present a complete definition about titanium dioxide , its physical properties (structural, optical and electrical) and some applications of this oxide. In addition to the doping of TiO_2 and the different deposition methods to synthesize Cu doped TiO_2 thin films.

I – 1 – Transparent Conductive Oxides and its properties:

Various materials can be classified into three categories based on their band structures as shown in Figure 1. For metals, the valence band is only partly filled and the electrons can easily move. For ideal semiconductors and insulators, the valence and conduction band is separated by a band gap leaving the valence band completely filled and the conduction band empty. A completely filled band cannot conduct electricity since the mobility of the electrons will be zero because they do not have any vacant position to move into. For a semiconductor, the gap is small enough so that electrons can be exited to the conduction band by absorption of visible light or by absorption of thermal energy. In the excited state, the mobility will increase both in the conduction and valence band, and hence semiconductors become electronically active. Semiconductors can be converted into permanently electronically active materials by doping. A material is transparent to visible light if the band gap is higher than ~3 eV. The band gap of insulating materials is so large that the magnitude of excited electrons becomes negligible [1].

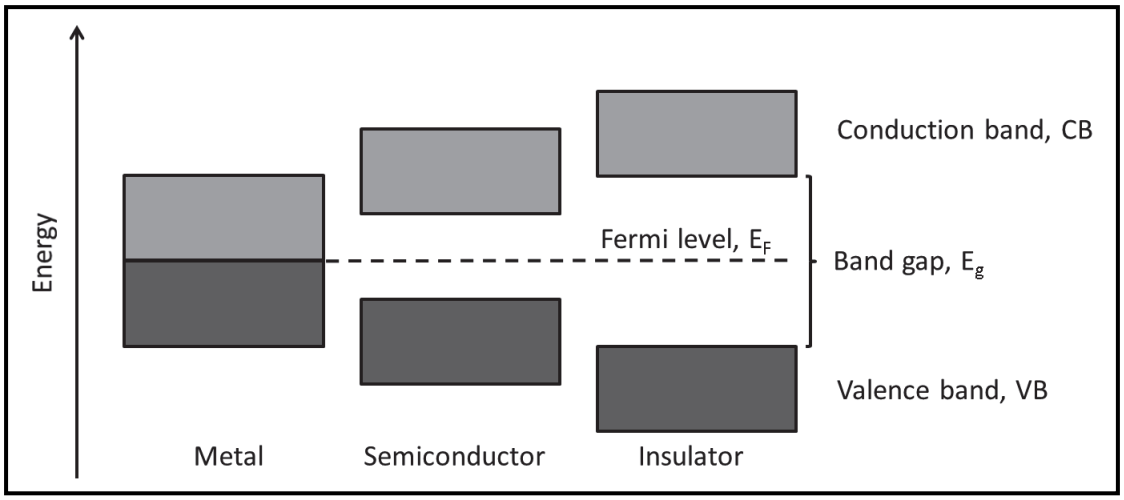

Fig.I.1 – A comparison of the band gaps of metals, insulators and semiconductors.

Transparent conductive oxides (TCOs) are the semiconductor materials which have high optical transmission at visible wavelength (390 –700 nm) and electrical conductivity close to that of metals. They also reflect near infrared and infrared (i.e., heat) wavelengths. This peculiar combination of physical properties is only achievable if a material has a sufficiently large energy band gap so that it is transparent to visible wavelengths ,i.e., $> \sim 3.0\ eV$, and also has a high enough carrier concentration ,i.e., $> \sim 10^{19} cm^{-3}$, with a sufficiently large carrier mobility $> \sim 1 cm^2 V^{-1} s^{-1}$ that the material can be considered to be a 'good' conductor of electricity .

In the most general sense TCO materials in combination of different metals or metal combinations as form of A_XB_Y (Where B is non-metal such as oxygen, A is metal or metal combination) or $K_zL_wM_p$ (Where M is non-metal, K and L metal or metal combination) as binary and ternary compounds respectively.

This characteristic behavior of TCOs mostly impossible in intrinsic stoichiometric oxides; nevertheless it may achieved both by producing them with a non-stoichiometric composition and introducing them with the feasible dopants [2] .

Band gap > 3.1 eV ensures that visible light photons cannot excite electrons from the valence band (VB) to the conduction band (CB) .These transparent materials are thus made electrically conducting by the introduction of defects (Mostly Oxygen deficiency) and extrinsic dopants into the system. TCOs can be classified as n-type or p-type, according to the defects and type of conduction of the material. These defects form split off acceptor (unoccupied) levels above the valence band maximum (VBM) in the case of p-type conduction, and donor (occupied) levels below the conduction band minimum (CBM) in the case of n-type conduction [2, 3].

N-type TCOs (SnO_2, ZnO, In_2O_3 etc) are already utilized in a range of technological applications. However p-type TCOs have proved to be harder to manufacture. Most of the wide band gap binary oxides have valence bands dominated by O 2*p* states. Hence on acceptor formation, the acceptor states (holes) are localized on oxygen ions, leading to low conductivity. Designing p-type TCOs with good conductivity has therefore still remains as a major challenge for materials scientists [3].

I – 1 – 1 – Application of TCOs:

TCO's have diverse industrial applications, some of the actual and potential applications of TCO thin films include:

(i) transparent electrodes for flat panel displays; (ii) transparent electrodes for photovoltaic cells; (iii) low emissivity windows; (iv) window defrosters; (v) transparent thin films transistors; (vi) light emitting diodes; and (vii) semiconductor lasers. As the usefulness of TCO thin films depends on both their optical and electrical properties, both parameters should be considered together with environmental stability, abrasion resistance, electron work function, and compatibility with substrate and other components of a given device, as appropriate for the application [4].

I – 2 – Titanium dioxide:

Titanium dioxide, also known as titanium (IV) oxide or Titania belongs to the family of transition metal oxides, is the naturally occurring oxide of titanium, chemical formula TiO_2 [5] . Like other metal oxides, it is hard, thermally stable and chemically resistant. Since the early twentieth century it has been produced commercially as a pigment and whitener [6] . TiO_2 exists naturally in three crystalline forms; anatase, rutile and brookite [5].

I – 3 – Titanium dioxide properties:

I – 3 – 1 – TiO_2 Structural properties:

Crystalline titanium dioxide can exist in different crystallographic arrangements, but all of them contain an octahedrally coordinated titanium atom. They only differ from each other in the way the octahedral atoms are bound together [7].

Three of these phases exist as naturally occurring polymorphs, anatase, rutile and brookite [7]. Where anatase and rutile are in tetragonal structure and brookite is orthorhombic. [8]. Anatase is a metastable phase that contains four shared edges per octahedron (the highest condensation of TiO_6 octahedral) and it shows photo catalytic behavior with response to ultraviolet photons [8] , it can be obtained in mineral form, but contains natural impurities including oxides of calcium, magnesium, sodium, iron and copper [7]. The rutile is the thermodynamically most stable phase at all temperatures and is formed by sharing two edges per octahedron (the lowest condensation of TiO_6 octahedral) with the largest index of refraction. Rutile is good for electronic components because of better conductivity than other phases. Brookite is the most distorted & unstable phase and shares three edges per octahedron, due to this, only anatase and rutile crystal can be utilized for technological point of view [8].

The metastable anatase and brookite phases convert irreversibly to rutile phase on heating above 600°C to 800°C temperature [9].

In all of TiO_2 phases, each titanium atom is surrounded by six oxygen atoms, leading to more or less distorted TiO_6^{2-} octahedrons. Crystal structures differ by the distortion of each octahedron and by the assembly patterns of the TiO_6^{2-} units. For the rutile structure, each octahedron is connected with 10 neighbors (two sharing edge oxygen pairs and eight sharing corner oxygen atoms), while for the anatase and brookite structures, every moiety is in contact with eight neighbors (four sharing an edge and four sharing a corner) as shown in Figure.2 Three dimensional TiO_2 network is obtained from a mixture of corner-sharing and edge-sharing octahedral units [11].

Table.I.1 – Crystal structure properties of TiO_2 [10].

Properties	Rutile	Anatase	Brookite
Crystal structure	Tetragonal	Tetragonal	Orthorhombic
Ti-O bond length (Å)	1.937(4) 1.965(2)	1.949 (4) 1.980 (2)	1.87-2.04
O-Ti-O bond angle	77.7° 92.6°	81.2° 90.0°	77.0°-105°
Lattice constant (Å)	a = 3.784 c = 9.515	a = 4.5936 c =2.9587	a = 9.184 b = 5.447 c = 5.154
Space group	$I4_1/amd$	$P4_2/mnm$	Pbca
Molecule	2	2	4
Density (g cm^{-3})	3.79	4.13	3.99
Volume / Molecule (Å^3)	34.061	31.2160	32.172

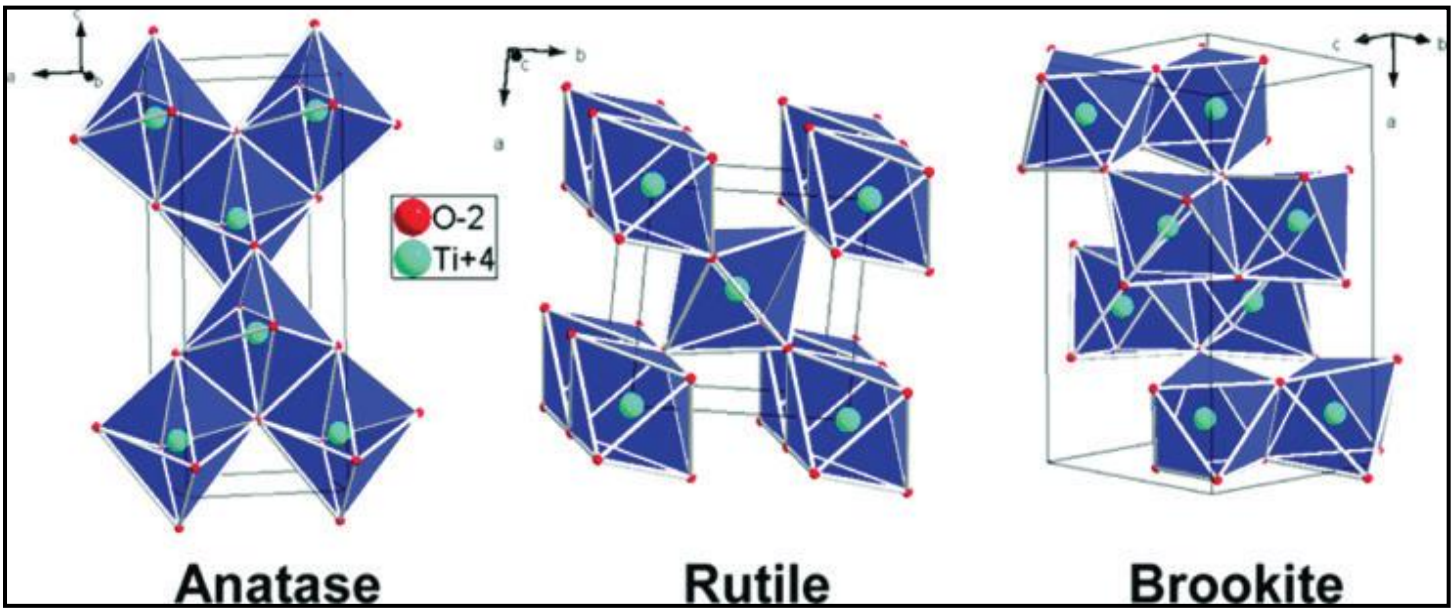

Fig.I.2 – Rutile, anatase, and brookite unit cells, all showing octahedral titanium coordination. Gray and red atoms correspond to Ti^{4+} and O^{2-}, respectively [11].

I – 3 – 2 – TiO_2 Optical properties:

TiO_2 is presented as a semiconductor material with a wide forbidden band (band-gap). The gaps in Rutile, Anatase and Brookite are 3 eV, 3.2 eV and 3.1 eV respectively. The band gap (Eg) is between the valence band (corresponding to the O 2p orbital) and the conduction band (corresponding at orbital Ti 3d). These gap values give rise to transitions corresponding to photons located in the ultraviolet range [12] .

In the visible range titanium dioxide has a high refractive index n. Of the three stable crystalline phases, Rutile has the largest index ($n \approx 2.66$) which is higher than that of the anatase one ($n \approx 2.54$). This combined with a high visible light scattering coefficient; make the Rutile phase suitable for use as a white pigment for the industry (paints, food coloring or pharmaceutical ...) [9].

The transmittance of TiO_2 in the visible range associated with an absorption edge around 0.42 μm leads to a high absorption in the ultraviolet which gives it excellent properties such as protective layer from UV, main active component of solar cells…etc [9] .

I – 3 – 3 – TiO_2 Electrical properties :

Since TiO_2 is a semiconductor, increasing the temperature causes increase in conductivity and even sensitive to any oxygen deficiency, will lead to have n-type semiconductor [8].

Despite the fact that the mobility of charge carriers is the highest in rutile due to better crystallinity, anatase exhibits more effective use of charge carriers in the reactions since it possesses more defect sites such as oxygen vacancies, which serves as active reaction centers. TiO_2 anatase is an example of n-type semiconductor with possession of dominant native defects (often oxygen vacancies), which can be formed its preparation [13].
The dielectric constant of rutile phase is an average of 114 and anatase of 40 promising material for gate dielectric in MOSFET type transistor and also for the manufacturing of capacitors.[8]

I – 4 – Doping of TiO_2 :

TiO_2 has a wide band-gap (3.2 eV), and can only absorb ultraviolet (UV) light. This limits the use of TiO_2 in large scale industrial applications notably, since solar light contains only 4-5% UV radiation. Therefore, around 15 years ago, researchers have directed their efforts to modify TiO_2 to allow activation by visible light, and at the same time introduce highly reactive sites on the surface via several modifications such as:

- Doping TiO_2 with transition element ions: the aim of this modification is to reduce the band gap of TiO_2 by incorporating small amounts of transition metal ions into the lattice of TiO_2, such as ionic forms of Cr, V, Fe and Cu.
- Promoting TiO2 with metallic nanoparticles: metallic nanoparticles (e.g. Pt , Rh , Ru and Pd) act as an electron 'beacon' (reducing electron/hole recombination), as well as catalytic center for reduction reactions, such as reduction of oxygen.
- Doping TiO2 with anions: Br, F, I, S, N, C. The purpose of this method, is to create intra-band energy levels allowing visible light absorption [14].

In this thesis, the doping effect of titanium dioxide by copper (Cu-TiO_2) on the optical properties is studied.

I – 4 – 1 – Copper properties:

Copper is a non-ferrous base-metal and its average concentration in the earth's crust is about 50 ppm (parts per million). The average minimum exploitable grade for a copper deposit is 0.4% which equates to a concentration factor of around 80 based on average crustal abundance. Copper occurs naturally in all plants and animals, as it is an essential element for all known living organisms.

Copper is classified as a noble metal, like gold and silver, and as a result can be found in its elemental or 'native' form in nature .It is one of the transition metals in the periodic table which means it can also form compounds, such as chalcopyrite the main copper ore ($CuFeS_2$), and copper ions (Cu^+ or Cu^{2+}) in solution. Copper metal has a characteristic reddish brown color, with a metallic luster on fresh surfaces. However, it quickly oxidizes in air, a feature of all base-metals. Copper is relatively soft (2.5–3.0 on Moh's scale of hardness). Other physical properties are summarized in Table 2 [15].

Table.I.2 – Copper properties [15].

Symbol	Cu	
Atomic number	29	
Atomic weight	63.546	
Density at 293 K	8960	kg/m^3
Melting point	1083	°C
Boiling point	2567	°C
Specific heat capacity at 293 K	386	J/kg
Electrical Conductivity	100	% (International Annealed Copper Standard)
Electrical conductivity at 293 K	5.98×10^7	$Ohm^{-1}\ m^{-1}$
Electrical Resistivity	1.673×10^{-8}	Ohm m

I – 5 – TiO_2 Applications :

I – 5 – 1 – Pigment:

Titanium dioxide in all its phases has one of the highest refractive indices of any know material (average n = 2.5). This leads to high reflectivity from the surfaces. Thus, when

deposited as a thin film, its refractive index and color make it an excellent reflective optical coating for dielectric mirrors. The powder from TiO2 is used as coloring agent in paints, inks, plastics, paper, synthetic fibers, rubber, painting colors and crayons, ceramics, electronic components, candy coating, glazed fruit, coloring of skim milk and flour, cosmetics, sun tanning lotions, and toothpaste. It is the most important pigment in the world, accounting for approximately 70% of total volume [14]. TiO_2 when used as a pigment, it is called titanium white, Pigment White 6, or CI 77891 [5].

I – 5 – 2 – Photocatalysis :

After Fujishima and Honda discovered the photocatalytic splitting of water on TiO_2 Electrodes in 1972, this oxide was introduced in the field of photocatalysis [16].

Photo-catalysis is the composing of photochemistry and catalysis with both light and a catalyst being desired to onset or precipitate a chemical conversion. The photo-catalytic process starts with the absorption of electromagnetic radiation, which excites an electron from the valence band to the conduction band, leaving a hole in the valence band. (Fig.3) is a schematic representation of this process. In this process UV light irradiation is used by photon energy equal to or greater than TiO_2 band gap energy ($h\nu \geq 3.20$ eV at $\lambda \leq 380$ nm); electron-hole pairs (The charge carrier) are generated . The negatively charged electron moves from the valance band (VB) to the conduction band (CB) leaving behind the positively charged hole. Then, the electron and hole take part in reduction oxidation reactions with species that are adsorbed on the surface of TiO_2, such as water, hydroxide (OH^-) ions, organic compounds or oxygen. The valence band hole (h^+) is highly oxidizing while the conduction band electron (e^-) is highly reducing. The charge carrier h^+ oxidizes H_2O or OH^- ion to the hydroxyl radical ($OH^\bullet$) that is a highly potent, non-selective oxidant. It easily attacks pollutants adsorbed at the surface of titanium dioxide or in aqueous solution degrading them to H_2O and CO_2. On the conduction band (CB) the electron reduces adsorbed oxygen (O_2) species to superoxide ($O_2^\bullet$), then undergoes a series of reactions to give the $OH^\bullet$ radical. The reaction of these radicals with organic substance, environmental pollutants or harmful microorganisms results in the decomposition of the latter. In a case where the above discussed processes do not occur, recombination of the charge carriers results and energy is released in the form of heat. This causes great reduction in TiO_2 photocatalysis efficiency .Electron-hole recombination is reaction competing with hole-donor and electron-acceptor electron-transfer reactions. Recombination can occur either in the semiconductor bulk or at the surface resulting in the

release of heat (or light) and is detrimental for the photocatalytic activity as the redox properties of the semiconductor are quenched [5].

TiO_2 has the potential to purify and treat waste and potable water as well as in improving indoor air quality. Hazardous organic compounds such as aromatics, halo-aromatics, aliphatics, dyes, dioxins, and other contaminants are introduced by pharmaceutical, textile, agricultural, and food industries to the environment. Many of these toxins could be degraded to harmless compounds (e.g. CO_2, H_2O) through photocatalytic reactions. The bactericidal effect of this oxide under UV radiation gives TiO_2 the ability to be used as a self-sterilizing surface in hospitals and clinical centers. Amphiphilic properties of UV-irradiated TiO_2 surfaces, related to its photocatalytic properties, enable the TiO_2 coated surfaces to act as anti-fogging and self-cleaning materials. The medical applications of the photocatalyst TiO_2 such as catheter antibacterial coatings and antitumor agents, to kill cancerous cells, have been studied in the past decade. The different applications of TiO_2, as a photocatalyst, are shown in Table 3 [16].

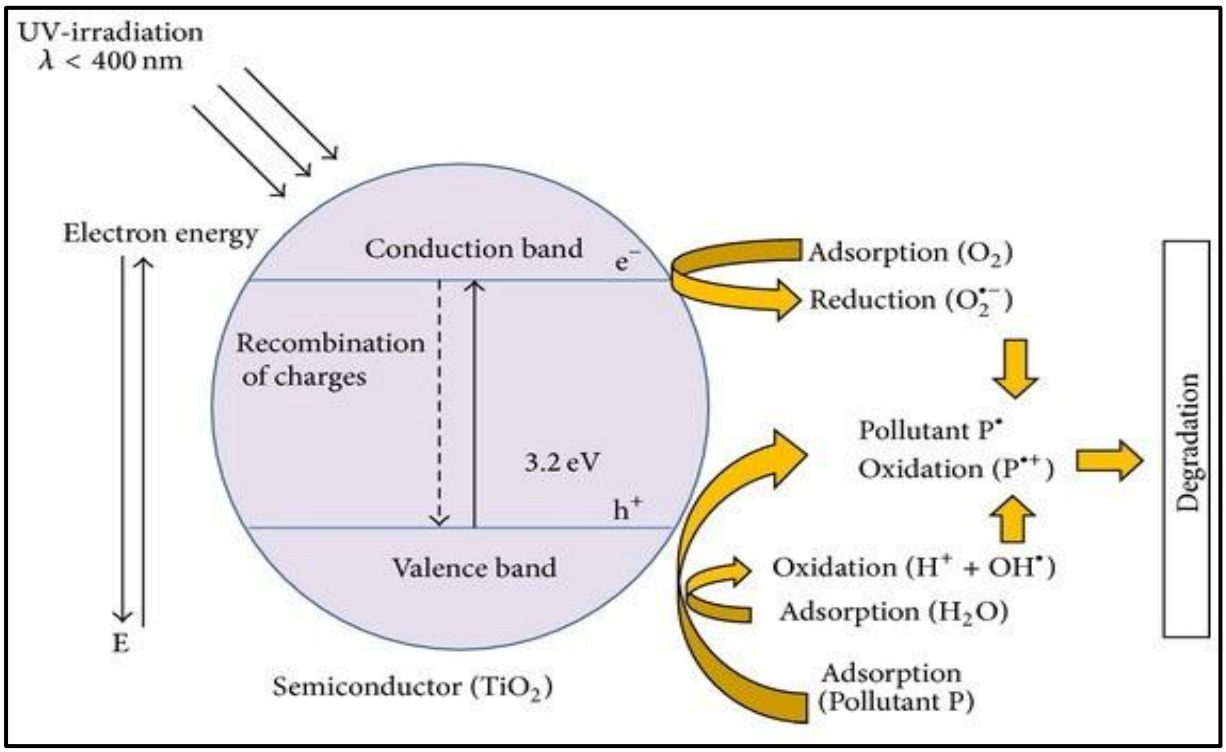

Fig.I.3 – Principal photo-catalytic process in the TiO_2 particles [5].

Table.I.3 - Different applications of TiO_2 as a photocatalysis [16].

Property	Application
Self-cleaning	Exterior tiles, kitchen and bathroom components, interior furnishings, plastic surfaces, aluminum siding, building materials and curtains, paper window blinds
	Translucent paper for indoor lamp covers, coatings on fluorescent lamps and highway tunnel lamp cover glasses
	Tunnel wall, soundproofed wall, traffic signs and reflectors
	Tent material, cloth for hospital garments and uniforms and spray coatings for cars
Air purification	Room air cleaner, photocatalyst-equipped air conditioners and interior air cleaners for factories
	Concrete for highways, roadways and footpaths, tunnel walls, soundproof walls and building walls
Water purification	River water, ground water, lakes and water-storage tanks
	Fish feeding tanks, drainage water and industrial wastewater
Antitumor activity	Endoscope-like instruments
Self-sterilising	Tiles to cover the floor and walls of operating rooms, silicone rubber for medical catheters and hospital garments and uniforms
	Public rest rooms, bathrooms and rat breeding rooms

I – 5 – 3 – Gas Sensor:

TiO_2 is an n-type semiconductor due to donor like oxygen vacancies. Akbar et al. reported that the sensing mechanism of anatase TiO_2 based carbon monoxide (CO) sensor involves CO adsorption and ionization on the titania surface and not an oxidation-reduction type reaction as observed in most oxide-based sensors. The behavior of anatase film can be explained based on the oxygen vacancies. Since a resistance decrease with concentration is the typically more favored response for gas sensor operation, n-type semiconductors are generally preferred over p-type. In stoichiometric n-type oxides, CO can inject electrons into the conduction band which result in an increase in the conductivity of the material. Therefore, the CO interacts

directly with the oxide rather than with the adsorbed oxygen .The change in the stoichiometry of TiO_2 can affect the electrical conductivity of the material as a function of the environmental oxygen activity at elevated temperatures. Three different mechanisms have been reported at higher temperature as reported by Dutta et al [16].

Mechanism-1:

O_2 (gas) $\longrightarrow$ O_2 (ads)

O_2 (ads) + e^- $\longrightarrow$ O_2^- (ads)

CO (gas) $\longrightarrow$ CO (ads)

$2CO\ (ads) + O_2^-\ (ads) \xrightarrow{\text{adsorbed intermediate}} 2CO_2\ (ads) + e^-$

CO_2 (ads) $\longrightarrow$ CO_2 (gas)

Mechanism-2:

O_2 (gas) $\longrightarrow$ 2O (ads)

CO(gas) $\longrightarrow$ CO (ads)

$CO\ (ads) + O\ (ads) \xrightarrow{\text{adsorbed intermediate}} CO_2\ (ads)$

CO_2 (ads) $\longrightarrow$ CO_2 (gas)

O_2 (ads) $\longrightarrow$ O_2 (gas) + V_O^{2+} + $2e^-$

Mechanism-3:

$TiO_2 + CO\ (gas) \longrightarrow TiO_2(CO)_{ad}$

$TiO_2(CO)_{ad} \longrightarrow TiO_x$ (adsorbed intermediate) $\longrightarrow TiO + O_2$ (gas)

$Ti^{2+} \longrightarrow Ti^{4+} + 2e^-$

$TiO + 1/2\ O_2\ (gas) \longrightarrow TiO_2$

Mechanism-1 suggests that the adsorption of oxygen at the surface defects can lead to the formation of species O^{2-} (and other oxygen containing species depending on the temperature). This leads to formation of dipole charge layers. In the presence of a reducing gas such as CO reaction at the grain surface leading to CO_2 formation liberates free electrons in the depletion layer, thereby reducing the resistance at the interface and this forms the basis for the sensing mechanism. Mechanism-2 suggests that a reaction occurs between CO and adsorbed oxygen. The resistance change occurs because of the

correspondence between O (ads) and the electron concentration. Mechanism-3 involves direct reduction of Ti^{4+} on the anatase surface. After CO_2 is desorbed, the extra electrons associated with the reduced Ti are distributed through the lattice, resulting in a decrease in the resistance. Oxygen can re-oxidize the site, resulting in the regeneration of the starting material [16].

The advantage of the TiO_2 gas sensor is that it has extraordinarily high sensitivity and this makes the design of the associated electronics quite simple provided that only alarm or crude monitoring facilities are desired [16].

I – 5 – 4 – Dye-sensitized solar cells (DSSC) :

DSSCs are based on dye-sensitization of a wide band gap semiconductor. In TiO_2-based DSSC, TiO_2 nanomaterials are covered with an organo-metallic dye immersed in an electrolyte containing a redox couple. The anode is composed of semiconductor with a transparent conducting electrode. The cathode is generally made of platinum or carbon.

In TiO_2-based DSSC, the light absorption and the charge separation functions are separated. When light is shined on the DSSC, the dye molecules interact with the photons and electrons are excited to a state that is energetically higher than the conduction band edge of the TiO_2. As a result, electron-hole pairs are generated in the dye. Electrons are injected into the conduction band of semiconductor, while the holes left in the dye are rapidly reduced by electrolyte, thus preventing recombination of the electrons and holes.

Electrons travel through the semiconductor to the electrode, the external load and finally to the counter electrode where they reduce the electrolyte. The TiO_2 are important not only because of the large amount of dye that can be adsorbed on the very large surface but also for another two reasons: (a) they allow the semiconductor small particles to become almost totally depleted upon immersion in the electrolyte (allowing for large photovoltages) and (b) the proximity of the electrolyte to all particles makes screening of injected electrons, and thus their transport, possible [17] .

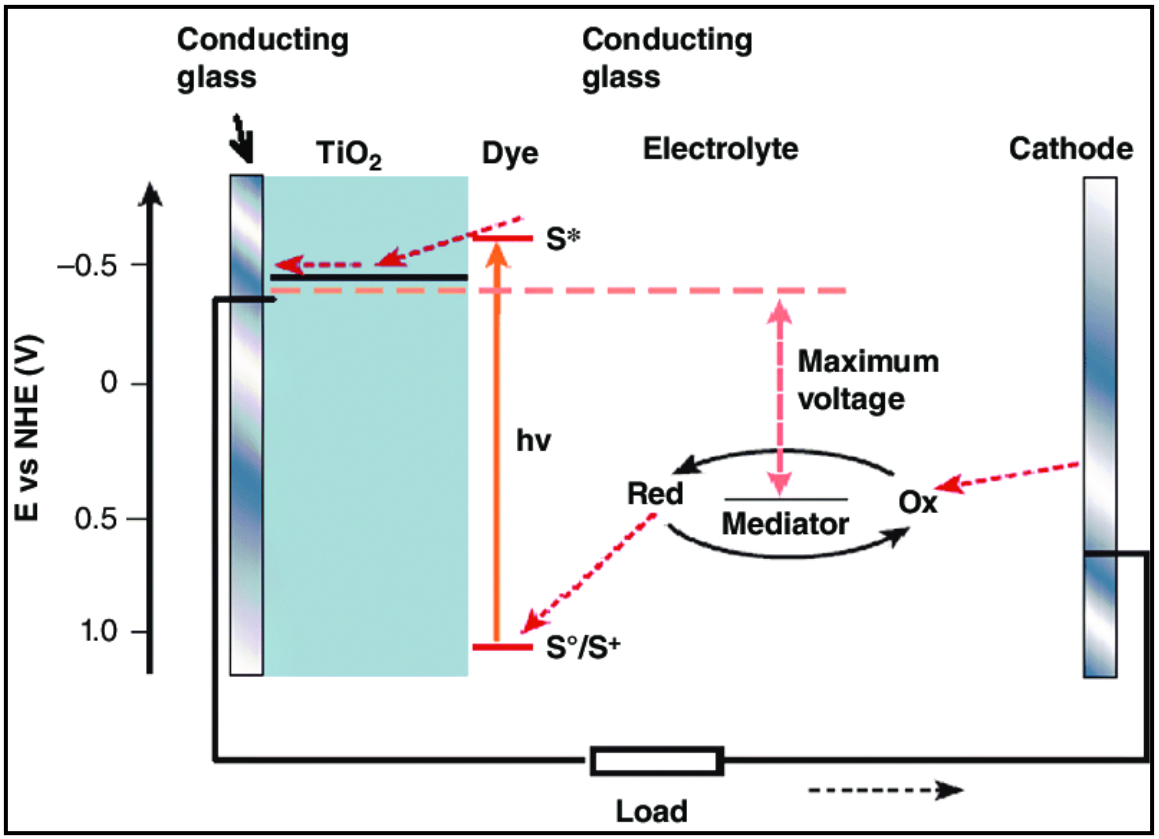

Fig.I.4 – Energy diagram of dye-sensitized solar cell [18] .

I – 6 – Deposition methods of Cu doped TiO_2 thin films:

Cu metal is found to be one of the most considerable elements which reduces the band gap energy of pure TiO_2 and makes it a visible light active material. Numerous works on the applications of Cu doped TiO_2 thin films have been reported [19] . Among those works are the following:

I – 6 – 1 – Hydrothermal method:

Hydrothermal processing is a non-conventional method to obtain nanocrystalline inorganic materials. A direct precursor-product correlation exists allowing the tailoring of almost any materials synthesis without the presence of further structure directing agents. In short, the synthesis method uses the solubility in water of almost all inorganic substances at elevated temperatures and pressures, and subsequent crystallization of the dissolved material from the fluid [20] . Using hydrothermal method Li Zhou et al [21] synthesized Cu-doped TiO_2 powders to study the influence of copper dopant with different concentrations on the band gap energies of TiO_2 nanoparticles to improve the performance of dye sensitized solar cells (DSSCs) . The pastes prepared from the Cu-doped TiO_2 powder were printed onto

fluorine-doped tin oxide conductive glass and used as photoanode semiconductor materials into dye N719 sensitized solar cells. The results of spectroelectrochemical measurement shows that the conduction band edge of TiO_2 moves to lower position after doping with Cu. The device based on 1.0% Cu–TiO_2 yields an overall energy conversion efficiency (η) of 6.12%, a short circuit current density (J_{sc}) of 13.11 mA cm^{-2} , a open circuit voltage (V_{oc}) of 0.73 V, and a fill factor (FF) of 0.64, indicating a 20% improvement in DSSCs performance.

I – 6 – 2 – Atmospheric-pressure thermal plasma method :

The fabrication process affects the purity and surface properties of the resulting TiO_2 nanoparticles, which subsequently influence the photocatalytic properties. Generally, liquid synthesis methods require multiple steps to prepare high-quality nanoparticles. Evaporation condensation using thermal plasma is advantageous because it develops nanoparticles with clean surfaces while modifying the catalyst surface in a single step [22]. Cheng-Yen Tsai et all [22] studied the Hg^0 removal effectiveness of Cu-doped TiO_2 in the presence of O_2, H_2O, and ultraviolet (UV) or visible light (VL), Cu-doped TiO_2 photocatalyst nanoparticles was prepared via a single-step process using an atmospheric-pressure plasma torch system. Degussa P-25 was thermally doped with Cu at Cu/(Cu + TiO2) ratios of 0–5 wt.% . The Hg^0 breakthrough tests indicated that the Cu-doped TiO_2 underwent appreciable Hg^0 removal under visible-light irradiation. Doped Cu effectively suppressed Hg reemission from the TiO_2 surface.

I – 6 – 3 – Inert gas condensation (IGC) method:

Nanostructured materials can be synthesized by the most widely inert gas condensation (IGC) technique, which can control the size, distribution and purity of the nanoparticles by using a thermal evaporation source, an electron beam evaporation device or a sputtering source in an inert gas atmosphere of argon or helium [23]. H A Ahmed et all [23] have investigated The band gap of thin films Cu-doped TiO_2 nanoclusters prepared using the inert gas condensation (IGC) technique at various Cu contents, UV-Visible absorption spectra indicated that the presence of Cu in the Cu-TiO_2 thin film samples had shifted the light absorbance to the visible region. Increasing Cu content decreased the band gap energy form 3.19 eV to 2.56 eV. The Cu-doped TiO_2 thin films produced by sputtering are expected to have high activities when used in photocatalytic applications.

I – 6 – 4 – Sparking method :

A sparking process is a material preparation method which is easy to use, low cost, rapid and uses non-toxic starting materials (e.g. Ti wire). This method produced semiconductor material in size of nanoparticle that made more surface area and is suitable for photocatalytic property [24]. Pattanasak Tipparak et all [24] studied pure and Cu-doped TiO_2 nanoparticles thin films of about 900 – 1200 nm thickness were deposited onto glass substrates by double tip sparking process. Ultraviolet-visible (UV-Vis) spectroscopy study is used to characterize the effect of copper dopant with different concentrations on the band gap energies of TiO_2 nanoparticles. The absorbance spectra indicated increase visible region and the band gap energy decreased with increasing copper contents.

I – 6 – 5 – Sol–gel dip coating method :

Sol–gel technique has emerged as one of the most promising techniques as this method produces samples with good homogeneity at low cost [25], high-purity materials can be synthesized at low temperatures. In addition, homogeneous multi-component systems can be obtained by mixing precursor solutions, which allows easy control of chemical doping for the prepared materials [27]. Many researches used dip coating method to synthesize Cu-doped TiO_2 thin films among them Zineb Essalhi et all [25] studied the effects of annealing temperature on the structural, optical and electrical properties of Cu-doped TiO_2 thin films, the films were deposited by sol–gel technique dip coating method using titanium tetrachloride $TiCl_4$ onto glass substrates. The structural data show that the films have a tetragonal structure. The optical data show that the Cu-doped TiO_2 thin films are transparent in the visible range and opaque in the UV region. The electrical characterization using 4-point probe indicates that the sample with the highest annealing temperature is less resistive. In another study R Vidhya et all [26] studied the influence of Cu concentration on the structural, morphological, optical and catalytic properties of TiO_2 thin films, titanium oxide (TiO_2) and Cu doped TiO_2 thin films of 2 µm thicknesses were deposited on glass substrates by sol-gel dip coating technique. The results imply that varying Cu content facilitates the possibility of modifying the structural, morphological and optical properties in TiO_2 thin films remarkably, the results also revealed that the measured optical band gap values of the prepared films decrease on increasing Cu concentration. The prepared thin films show improved crystallinity, increased surface area, large visible light response and proficient catalytic activity. Furthermore, the results support

in exploring potential applications of reusable Cu/TiO_2 thin films as a promising photocatalyst for commercialization. Weerachai SANGCHAY et all [27] investigated The effect of the Cu doping into TiO_2 thin films on the microstructure, photocatalytic activity and antibacterial behavior. Thin films of TiO_2 and TiO_2 doped with Cu coated on glass slides were prepared by sol-gel and followed by dip coating process. It was observed that higher Cu concentration gives better photocatalytic activity. With the highest dopant concentration investigated in this experiment (TiO_2-1.0Cu condition) the films show photocatalytic of 70 % and antibacterial activity of 100 %.

Rajendran Vidhya et all [19] studied the effect of prepared Cu-TiO_2 thin films' thickness (5, 7, and 9 dip coatings) towards their structural, surface morphological and optical properties, and the performance of multilayer coated Cu-TiO2 thin films on protecting soil beneficial microorganisms (Rhizobium and Phosphobacteria) from UV light radiation . The results proved that the thicker the prepared samples, the more will be crystalline Improvisation, UV absorbance enhancement and band gap reduction. Anti UV effect of high thickness Cu-TiO2 thin films shows high survival rate of microorganisms. This beneficial effect of Cu -TiO2 thin films can be employed in protecting constructive microorganisms and human skin from harmful UV radiations.

I – 6 – 6 – Spray pyrolysis method :

Spray pyrolysis is a cost effective, simple and efficient technique. This technique has the capability to produce large surface area, high quality adherent films with uniformity, easiness of doping, operates at moderate temperatures (100-500°C) that opens the possibility of wide variety of substrates, control of thickness, variation of film composition along with thickness and possibility of multilayer deposition [28]. Arunananthan Mathi Vathani et all [28] made a report about an effective uric acid (UA) electrochemical biosensor using Cu-TiO_2 electrode. Uric acid (UA) biosensor was constructed using Cu doped TiO_2 electrode in an electrochemical cell. TiO_2 and Cu-TiO_2 with various concentrations of Cu were deposited on glass substrates by spray pyrolysis technique. Good crystallinity and electrical, optical and surface properties of 0.05Wt% Cu TiO_2 film show that the film is good for fabrication of biosensor. The electrochemical response studies of Cu-TiO_2 electrode for detection of UA show high stability, with sensitivity of 3.81μA $mM^{-1}cm^{-2}$.this study implies that the constructed Cu-TiO_2 thin film based electrochemical biosensor act as a potential candidate for application in the detection of UA.

Chapter 2

Sol-Gel deposition method and characterization techniques

This chapter is devoted to a definition of sol-gel deposition method and then the followed experimental procedure to deposit pure TiO2 and Cu doped TiO2 thin films by means sol-gel dip coating deposition method , as well as certain thin film characterization techniques such as: x-ray diffraction (DRX) , scanning electron microscopy (SEM), UV-Visible spectroscopy. This study was carried out in the laboratory of physics of thin films and applications (LPCMA) University Mohamed Khider of Biskra.

II – 1 – Sol-Gel deposition method :

One of the most versatile methods to prepare pure and doped TiO_2 thin films is the sol-gel technique. It has become famous in the glass and ceramic fields because it offers many advantages, among which the possibility to control the stoichiometry and the homogeneity of the final product and it allows to work in mild and ambient atmosphere conditions [30]. The term sol-gel corresponds to the abbreviation "solution-gelation" [29]. Usually inorganic metal salts or metal organic compounds such as metal alkoxide are used as precursors. A colloidal suspension or a “sol” is formed after a series of hydrolysis and condensation reaction of the precursors. Then the sol particles condense into a continuous liquid phase (gel) [9].

a. Solution based on an inorganic precursor :

The aqueous solution of a mineral salt is used. In this solution, the cations M^{z+} are captured by polar molecules H_2O. A bond $(M – OH)^{(z-1)+}$ is formed when an electron from a saturated orbital σ is transferred to a lower energy orbital and not saturated. This results in fact in the following two partial reactions:

$$M^{z+} + (OH)^{-} \leftrightarrow (M–OH)^{(z-1)+} \qquad (II–1)$$

$$(M – OH)^{(z-1)+} \leftrightarrow (M = O)^{(z-2)+} + H^{+} \qquad (II–2)$$

We know that according to the aforementioned reactions that in an acid medium, by increasing the PH of the solution, one of the following two types of ligands can form:

- Ligand hydroxo : $(M – OH)^{(z-1)+}$
- Un ligand Oxo : $(M = O)^{(z-2)+}$

Condensation reactions involving the hydroxo ligands: $(M – OH)^{(z-1)+}$ lead to the formation of (M – OH – M) or (M – O – M) bonds. Note, however, that colloidal solutions and stable gels can be obtained by keeping the PH constant. This route is mainly used in industrial powder manufacturing processes [12].

b. Solution based on an organic precursor:

The most used organic precursors are metal alkoxides of generic formula M $(OR)_z$ where M denotes a metal of valence z and R denotes a radical of an alkyl chain - $(C_n H_{2n+1})$. The metal alkoxides must be of high purity and have high solubility in a wide variety of solvents. This condition of high solubility can generally only be achieved in organic solvents. The main advantage of using organic precursors is to allow a homogeneous and intimate molecular mixture of different precursors in order to produce glasses and ceramics with several components [12].

II – 1 – 1 – Chemical reactions of Sol-Gel method :

The mechanism of chemical reactions in the sol-gel method consists of two concomitant reactions :hydrolysis and condensation.

II – 1 – 1 – 1 – Hydrolysis reaction:

During the hydrolysis reaction, the alkoxide groups (OR) are replaced with hydroxyl group (OH) through the addition of water as shown in the equation below:

$$M(OR)_n + H2O \rightarrow M(OR)_{n-1}(OH) + ROH \qquad (II–3)$$

Although hydrolysis can occur without additional catalyst, it has been observed that with the help of acid or base catalyst the speed and extent of the hydrolysis reaction can be enhanced . The mechanism of hydrolysis of a metallic alkoxide M(OR)n (neutral medium, without additional catalyst) is given as follows [9] .

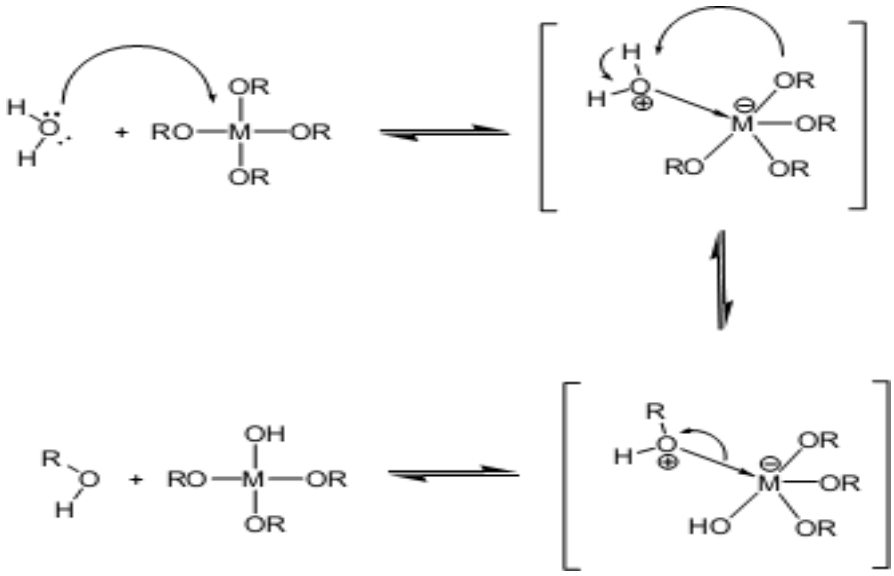

II – 1 – 1 – 2 – Condensation reaction :

The groups (HO−M $(-OR)_{n-1}$) generated during the hydrolysis react either with each other to give a molecule of water (oxolation) or with a molecule M of the alkoxy (−OR) to give an alcohol molecule (alcoxolation) and leading to the creation of the or each flight MOM

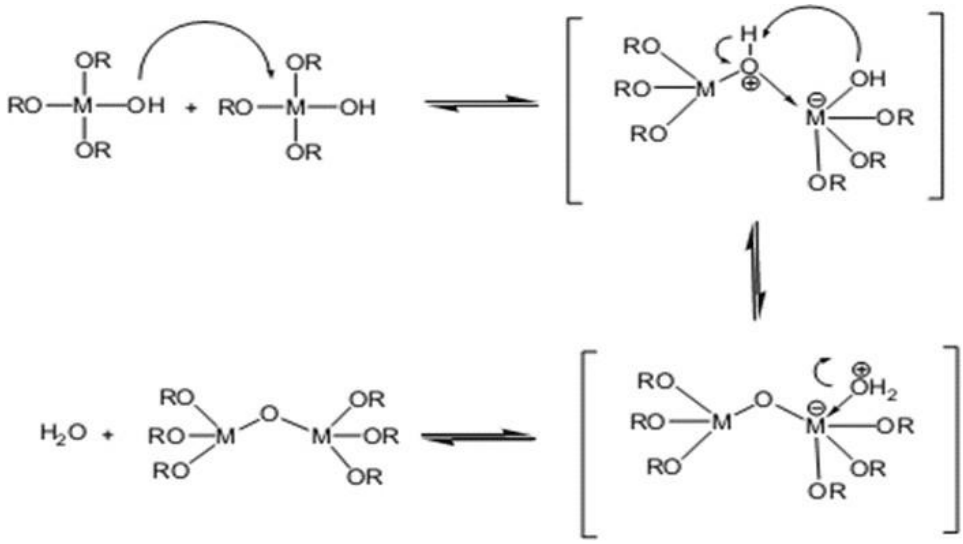

oxygen atom becomes a bridge connecting two atoms of the metal M. This leads to the formation of a gel that's its viscosity increases during time; this gel contains solvents and precursors which have not yet reacted. This process is governed by the following reactions at room temperature. The mechanism of oxolation of a metallic alkoxide $M(OR)_n$ [9] :

The mechanism of alcoxolation of a metallic alkoxide $M(OR)_n$ [9] :

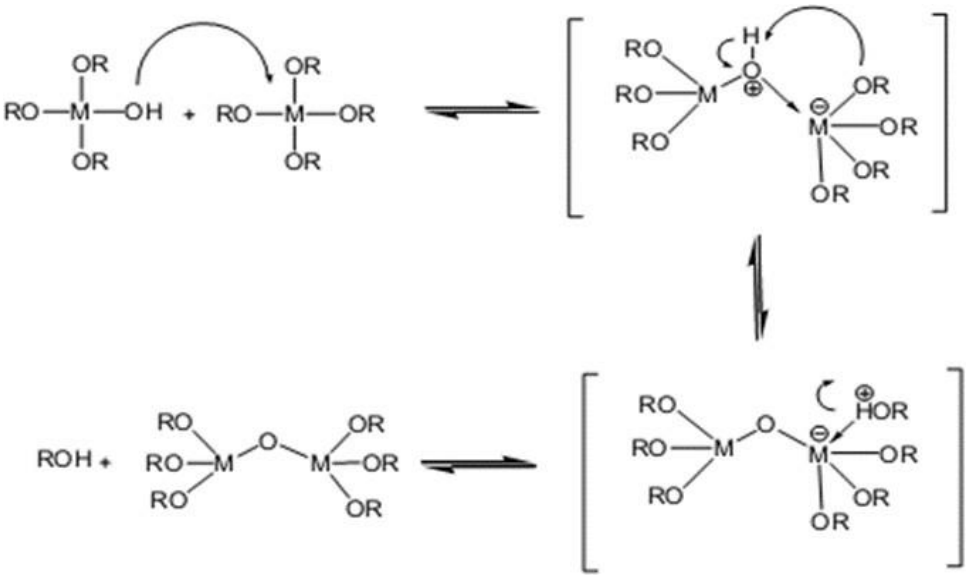

II – 1 – 2 – Different Sol-Gel deposition methods :

The most commonly used sol-gel deposition methods of thin films are dip-coating and spin-coating.

II – 1 – 2 – 1 – Dip-coating :

This technique consists of immersing the substrate in the precursor solution and removing it under very controlled and stable conditions to obtain a thin film of a regular thickness (fig.II.2). In general, the process can be separated into three important steps [29] :

Immersion & dwell time: the substrate is dipped in the precursor solution at a constant speed and followed by a certain dwell time to allow sufficient interaction time of the substrate with the solution.

Deposition: the substrate is pulled upwards at a constant speed (film deposition : Excess liquid will drain from the surface).

Evaporation: the solvent evaporates by hot drying to form the thin films which can also be treated by annealing at a high temperature to improve their crystallization .

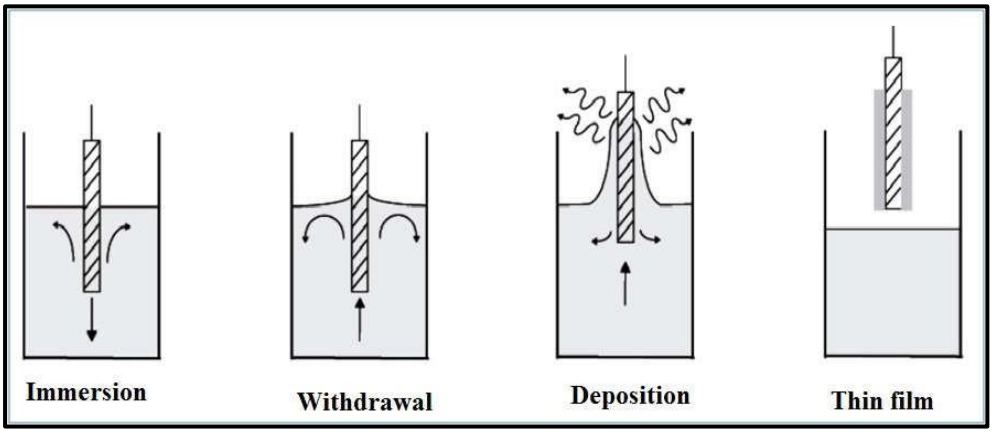

Fig.II.1 – The different stages of the dip-coating technique [29].

II – 2 – Experimental procedure:

II – 2 – 1 – Preparation of substrate:

II – 2 – 1 – 1 – Choose of substrate:

The Cu doped TiO_2 thin films were deposited on glass substrates, the choice of glass as a substrate is due to the following reasons:

- The thermal compatibility with TiO_2 which minimize the stress in the interface film/substrate [12].
- For their transparency which adapts well for the optical characterization of thin films in the visible region [12].

II – 2 – 1 – 2 – Cleaning of the substrate:

Substrate cleaning is an important process before deposition to obtain a good quality thin film and well adhered to the substrate, the substrates were cleaned according to the following steps :

- The substrates were rinsed with acetone for 10 min
- then rinsed with ethanol for 10 min.
- finally dried using dryer

Between each step the substrates are rinsed with distilled water.

II – 2 – 2 – Preparation of the solutions:

In order to prepare the solutions of pure TiO_2 and Cu doped TiO_2 the following components were used:

- Tetranium (IV) isopropoxide (Ti $(C_3H_5O_{12})_4$) TTIP as a precursor.
- Ethanol as a solvant.
- Acetic acid glacial as a catalyst.
- Copper II nitrate trihyrate (Cu $(NO_3)_2$ $3H_2O$) as a source of copper.

- **Pure TiO_2 solution :**

0.5 ml of acetic acid glacial was added to 2.25 ml of TTIP drop by drop under stirring for 15 min at room temperature, then 10 ml of ethanol added to the mixture and kept stirring for 2 h (when mixed with the Cu solution stirred just for 15 min) , finally a clear yellowish solution was obtained .

- **Cu doped TiO_2 solution :**

0.146 g , 0.073g and 0.0365 g of copper II nitrate trihyrate were added to 5 ml of ethanol and kept stirring for 15 min, then mixed with the pure TiO_2 solution and kept stirring for 2 h , finally three Cu doped TiO_2 solutions with bluish green color were obtained with different copper concentrations namely $3{,}404x10^{-5}$, $1{,}702x10^{-5}$ and $8{,}511x10^{-6}$ mol/l .

The properties of the chemicals used in the preparation of the solutions are shown in the following table:

Table.II.1 – Properties of the chemicals used in the preparation of solutions

	Precursor	**Catalyst**	**Solvent**	**Copper source**
Compound	Tetranium (IV) isopropoxide (TTIP)	Acetic acid glacial	Ethanol	Copper II nitrate trihyrate
Physical state	liquid	liquid	liquid	Solid powder
Molecular Formula	$Ti(C_3H_5O_{12})_4$	$C_2H_4O_2$	C_2H_5OH	$Cu(NO_3)_2\,3H_2O$
Density at 20 °C (g/cm^3)	0.96	1,048 - 1,050	0,790 - 0,791	-
Purity (%)	97	99.7	99.8	99 - 104
Molecular weight (g/mol)	284.22	60.05	46	241.60
Boiling point (°C)	232	-	78 - 79	-

II – 2 – 3 – Deposition of thin films:

HOLMARC dip-coating apparatus were used to deposit pure TiO_2 and Cu doped TiO_2 thin films onto glass substrates using the previously mentioned solutions at the laboratory of physics of thin films and application (LPCMA) – University of Biskra.

The principle work of this apparatus can be described as follows, The substrate is fixed in a movable holder and descends at a constant speed towards the solution, once the substrate is immersed in the solution, it remains for a few minutes, then it removed from the solution at a controlled speed , upwards to an infrared dryer to evaporate the most volatile solvents and finally the desired thin films were obtained.

Fig.II.2 – Dip coating apparatus

II – 2 – 3 – 1 – Experimental conditions :

In this work, the parameter which varied for the study of deposition of thin films of pure titanium dioxide and copper doped titanium dioxide is the concentration of copper $3{,}404x10^{-5}$, $1{,}702x10^{-5}$ and $8{,}511x10^{-6}$ mol/l and the fixed parameters are shown in the following table:

Table.II.2 – Fixed experimental conditions of the deposition of TiO_2 and Cu-TiO thin films

	Parameters	Reference
Dip speed	**5 mm/s**	-
Dip duration	**30 s**	[31]
Withdrawal speed	**4 mm/s**	-
Dry duration	**5 min**	[31]
Pre-heating tumperature	**100 °C**	[31]
Number of dips	**5**	[31]

The whole procedure for the preparation of TiO_2 and Cu doped TiO_2 thin films with the sol-gel dip-coating method can be summarized as shown in Figure.II.4 below:

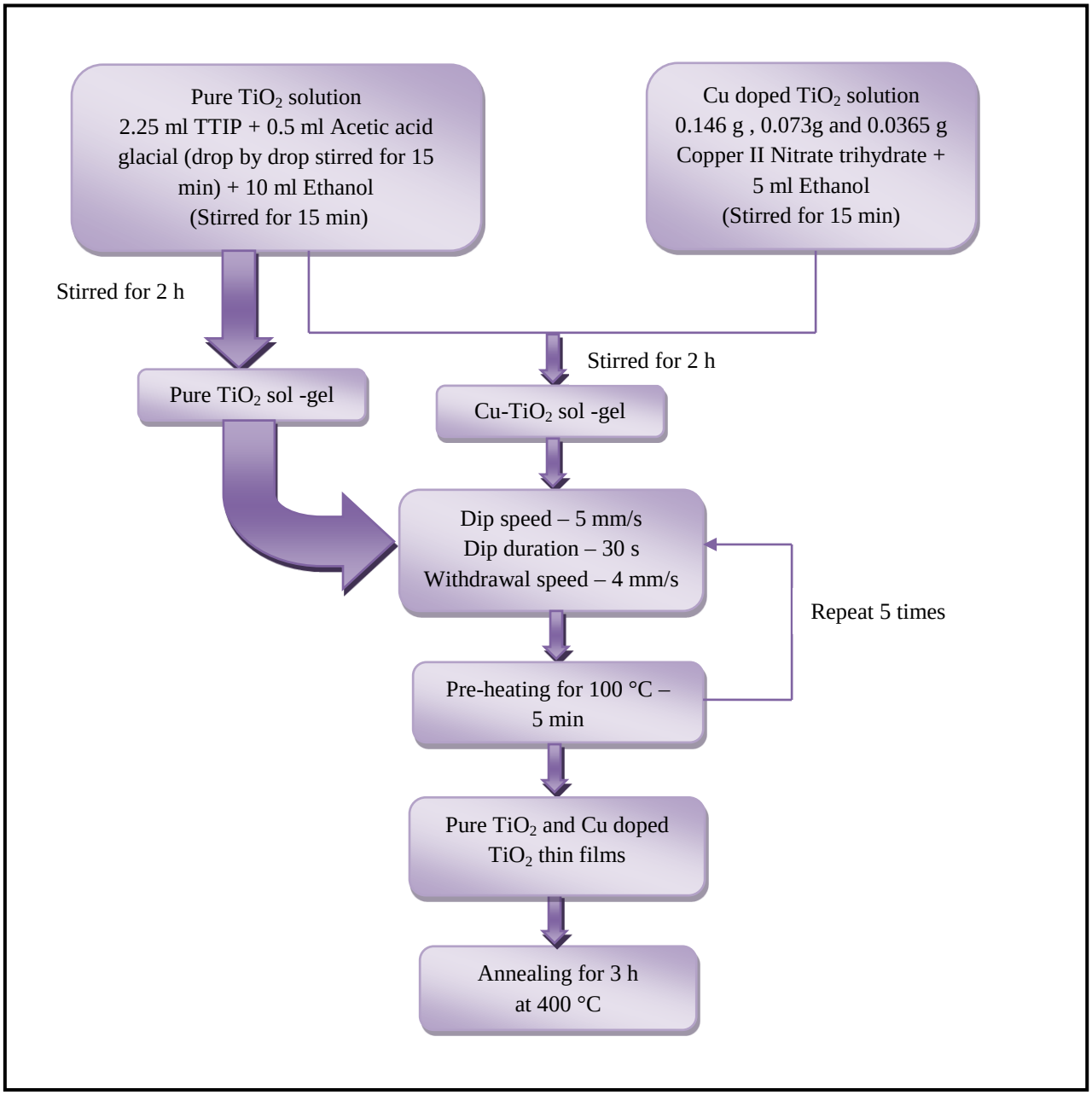

Fig.II.3 – The preparation of pure TiO_2 and Cu doped TiO_2 thin films by dip-coating

II – 2 – 3 – 2 – Adhesion test (tape test) :

An adhesive tape is applied to the film surface and pulled off again. The tape test is a subjective test which is not only dependent on the type of tape but also on the pull off velocity and the pull off angle. If the coating delaminates completely or partially bad

adhesion is given in each case (see Fig.II.5). If the coating adheres to the substrate it is not possible to decide if adhesion is moderate, good or very good [32].

In our case the prepared thin films adhesion was tested using tape test, the adhesion strength, it is considered "good" and the thin coating layer adhered to the substrate.

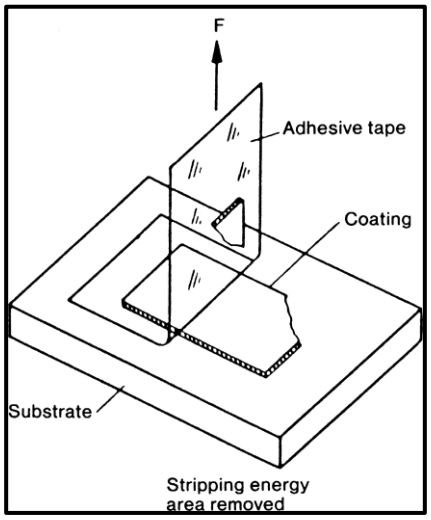

Fig.II.4 - Schematic of the tape test [32].

II – 2 – 3 – 3 – Annealing:

This is usually the most important process in the preparation of thin films; it allows a better crystallization (transition from amorphous to polycrystalline) and eliminates organic residues of precursors used in the solution [29], after drying the prepared thin films were annealed for 3 hours in an electric oven at 400 °C.

II – 3 – Characterization techniques of thin films :

Characterization is an important step in the process of preparation of thin films to analyze their physical properties. In this paragraph, we briefly recall the different characterization methods used in this study.

II – 3 – 1 – Structural characterization using X-Ray Diffraction (XRD):

The X-ray diffraction is a non-destructive structural analysis method for determining the crystal structure of materials in the form of bulk materials, powders or thin films. It is based on the Bragg law (figure.II.5) which gives the relation between the distances d_{hkl} between the crystallographic planes, the wavelength λ of the X-rays and the diffraction angle θ [29] :

$$2d_{hkl} \sin\theta = n\lambda \qquad \text{(II–4)}$$

Where:

d_{hkl} : the interplanar distance;

θ: X-ray incidence angle;

n: the order of diffraction;

λ: the wavelength of X-rays.

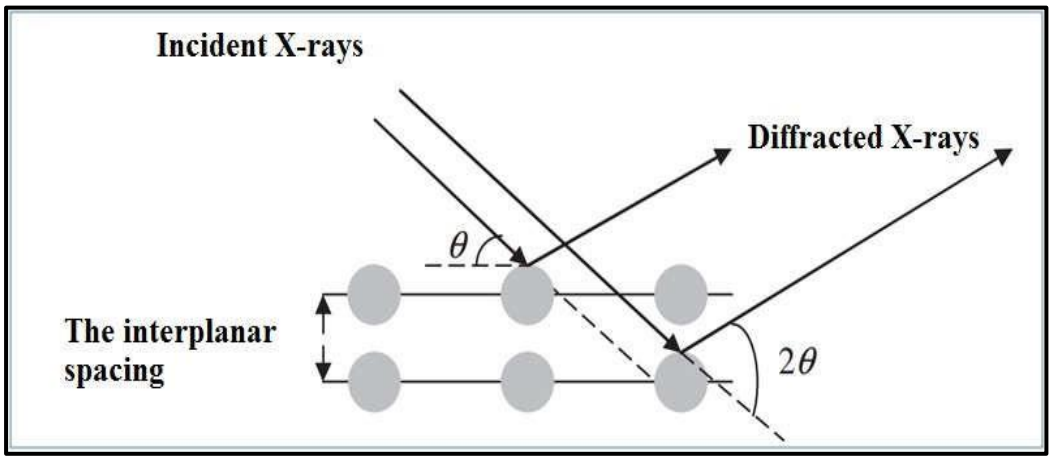

Fig.II. 5 – The Principle of Bragg Law [29].

This technique is based on the interaction of an X-ray beam monochromatic, emitted by a source, with the sample to be analyzed. A detector receives the beam diffracted by this sample and the intensity is recorded as a function of the diffraction angle 2θ. A diffraction peak corresponding to the considered family of planes obtained verified the Bragg law .The highlighted peaks must then be compared with the international tables of the JCPDS-ICDD files (Joint Committee of Powder Diffraction Standard International Center for Diffraction Data) . We can then, by comparison with its files, establish the diffracted planes and the orientation of the thin films produced [33].

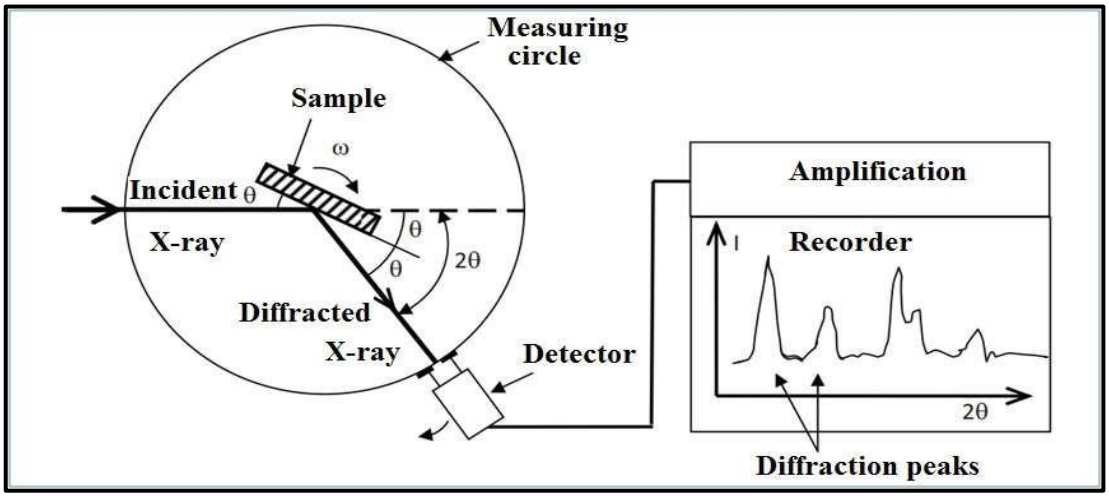

Fig.II.6 – Schematic diagram of an X-ray diffractometer [29].

The spectrum of X-ray diffractions makes it possible to know the different characteristics of a crystallized material, the orientation of the crystallites, the crystalline phases (peak position), the strain, and the crystallite size (D).

In this study, we used a X-Ray diffractometer "Rigaku Mini Flex 600" apparatus to characterize the structural properties of pure TiO_2 and Cu doped TiO_2 thin films.

Fig.II.7 – X-Ray diffractometer [34].

II – 3 – 2 – Morphological characterization using Scanning Electron Microscopy (SEM) :

Scanning electron microscopy (SEM) is an applicable technique for studying the surface of thin films. It makes it possible to give the general appearance of the films and to detect the presence of very fine droplets of solid material, their number and size. It can also give information on the growth mode of the film. Scanning microscopy involves putting a sample under vacuum and then bombarding it with a very fine electron beam. Indeed, the electron-matter interaction. To be detected, particles and radiation must be able to reach the surface of the sample. The maximum depth of detection, therefore spatial resolution, depends on the energy of the radiation. The sample must be conductive in order to be able to be observed at SEM. If it is insulating, it must first be metalized, that is to say, covered, for example, with a thin layer of carbon or gold [33]. The SEM apparatus used in our work is Tescan-Vega 3.

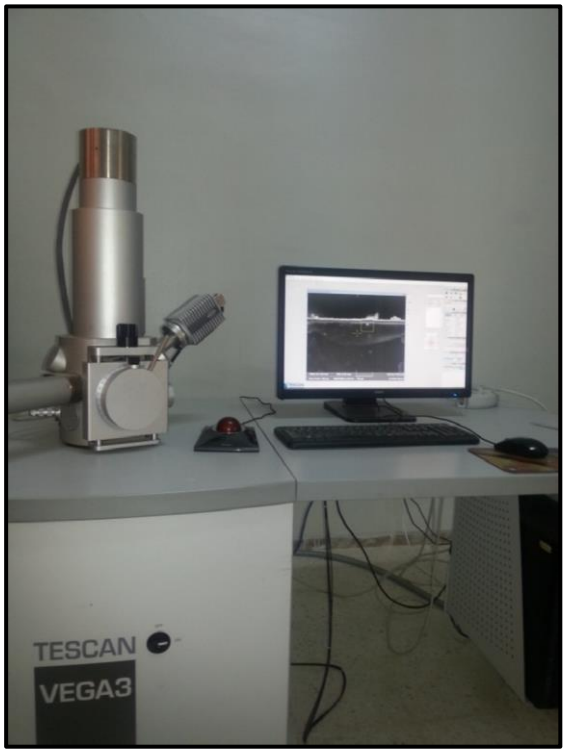

Fig.II.8 – The scanning electron microscopy [34].

II – 3 – 3 – Chemical composition using Energy dispersive X-ray spectroscopy (EDX) :

The X-ray spectroscopy emitted by an electron beam bombardment sample can be analyzed using the technique Energy Dispersive Spectroscopy (EDX), coupled with the SEM, the EDX detector makes possible to perform surface chemical, qualitative and quantitative analyzes with a penetration of about few micrometers, depending on the energy of the incident electron beam and the studied material [34].

II – 3 – 4 – Optical characterization using UV-Visible spectrophotometer :

Ultraviolet–visible spectroscopy (UV-Vis) is a method used to evaluate optical properties (such as reflectance, index of refraction, extinction coefficient) of a material through the measured spectral range. The instrument used for this evaluation is called spectrophotometer [35].

A first beam of light from a UV-Visible source such as tungsten filament (300-2500 nm), Deuterium arc lamp (190-400 nm), Xenon arc lamp (160-2,000 nm) is split by a prism or Diffraction grating. One beam pass through the sample while the other beam is used as reference (substrate) . The intensities of these light beams are then measured by electronic detectors and compared (as schematized in fig. II.10). the intensity of the reference beam, is defined as I_0. The intensity of the sample beam is defined as I.

The ratio between these two values $T = \frac{I}{I_0}$ is called transmittance, while the absorbance is defined as $A = \log\left(\frac{I_0}{I}\right)$ [35].

A double-beam UV-Visible Jasco V-770 spectrophotometer was used to obtain the transmittance spectrums of the prepared thin films.

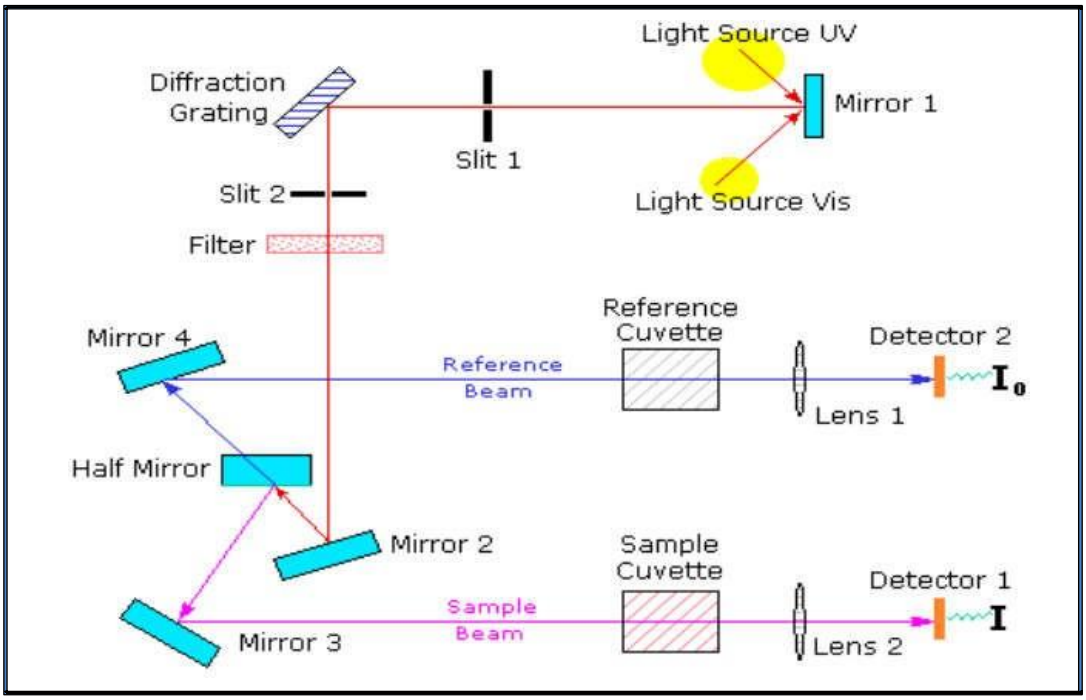

Fig.II.9 – Schematic representation of the UV-Visible spectrophotometer [29] .

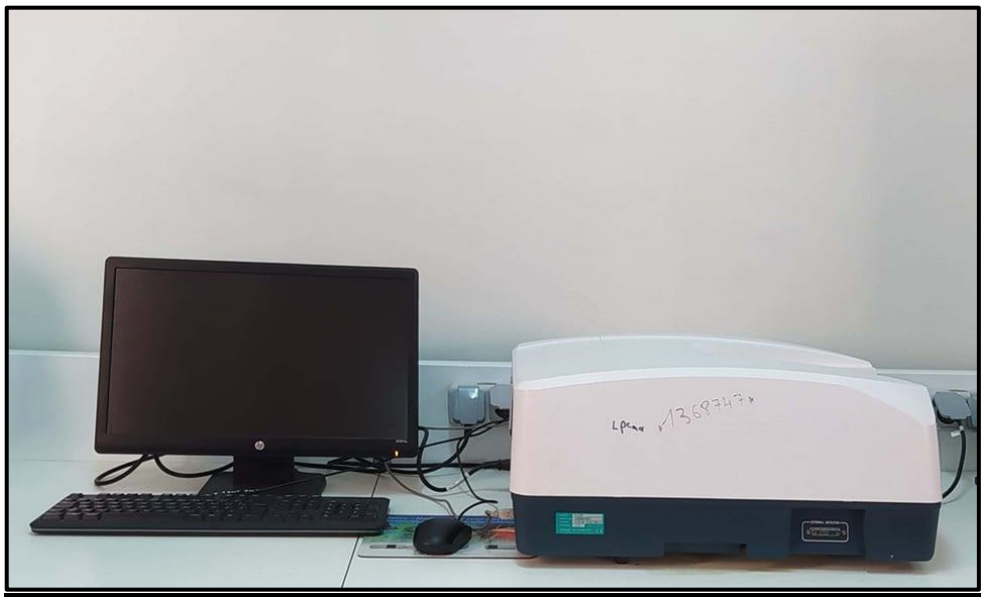

Fig.II.10 – UV-Visible spectrophotometer

II – 3 – 4 – 1 – Absorption coefficient:

If we have a spectrum of transmittance and the thickness d of a thin film we can determine the absorption coefficient by using the Bouguer-Lambert-Beer formula [29] :

$$T = e^{-\alpha d} \quad (II - 8)$$

In the case where the transmittance T is expressed in (%), the absorption coefficient is given by [29]:

$$\alpha = \frac{1}{d} \ln\left(\frac{100}{T(\%)}\right) \quad (II - 9)$$

Where:

T : is the transmittance,

d : the thickness of the layer,

α : is the absorption coefficient

II – 3 – 4 – 2 – Optical band gap :

The optical gap (Eg) is determined by using the Tauc equation [29]:

$$(\alpha h\upsilon) = A\left(h\upsilon - E_g\right)^n \quad (II - 10)$$

Where :

A : is a constant,

α : is the absorption coefficient,

hν : the energy of a photon .

E_g : the energy of the optical band gap.

n : is a number depends on the nature of optical transition, can obtain the values 1/2, 2, 3 and 3/2 for direct allowed, indirect allowed, direct forbidden and indirect forbidden transitions, respectively.

The value of the optical band gap can be estimate by ploting $(\alpha h\nu)^n$ versus hν and then extrapolating the linear region of the plot until it cross the hν axis (i.e. for $(\alpha h\nu)^n = 0$) , the intersection point is the value of the optical band gap E_g .

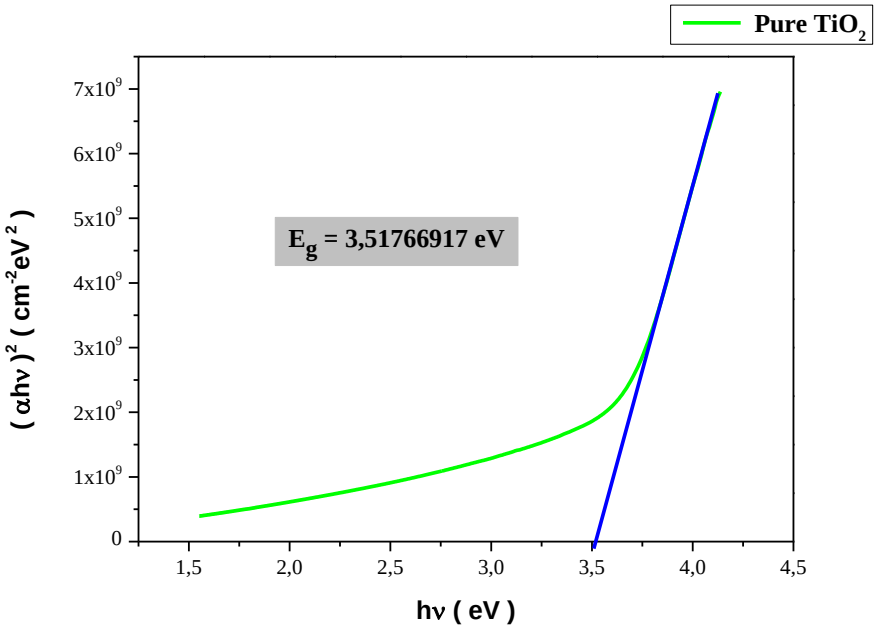

Fig.II.11 – Estimation of the value of the band gap of a TiO_2 thin film

II – 4 – Thickness measurement:

II – 4 – 1 – Surface profilometer :

Surface profilometer can measure profile of surface roughness, surface texture, surface waviness, surface step height, deposited thin film thickness, and so on by means of contacting and scanning a sharp stylus with a very small measurement force less than mN. Line scanning of a stylus on a rough substrate surface can change the height of stylus to be detected by a displacement sensor as shown in Fig.II.15.
Simple system of surface profilometer can offer a wide range of stylus scanning of area from micrometer scale to centimeter scale and can also offer a wide range of height measurement from nanometer or less up to micrometer depending on stylus tip diameter [36] .

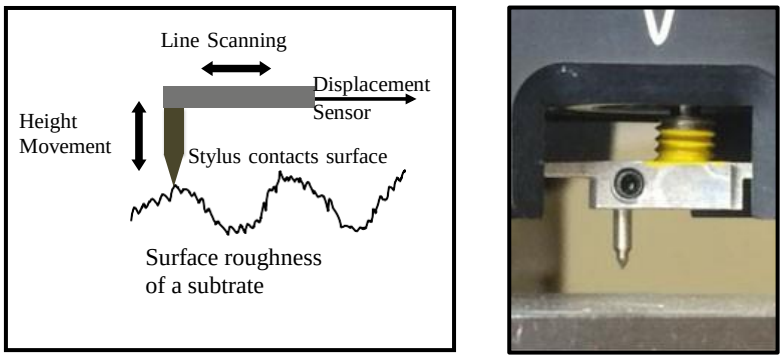

Fig.II.12 – Schematic and photograph of a surface profilometer [36] .

Surface profilometer consists of a stylus, a displacement sensor unit connected to a stylus, a substrate holder, a base plate with a line scanning system, a vibration isolation frame, a system controller with PC for line scanning speed and length, measurement and data

analysis, and so on as shown in Fig.II.16. Main unit of surface profilemeter is the displacement sensor consisting of a stylus with a linear variable differential transformer to detect displacement of a stylus with from sub-micrometer to a few tens of micrometers in diameter and with a controller for a stylus load adjustment. PC unit for total system control and data processing can show such surface profile parameters as an arithmetical mean deviation of roughness profile (Ra), a maximum height of roughness profile (Rz), a root mean square deviation of roughness profile (Rq) and so on [36]

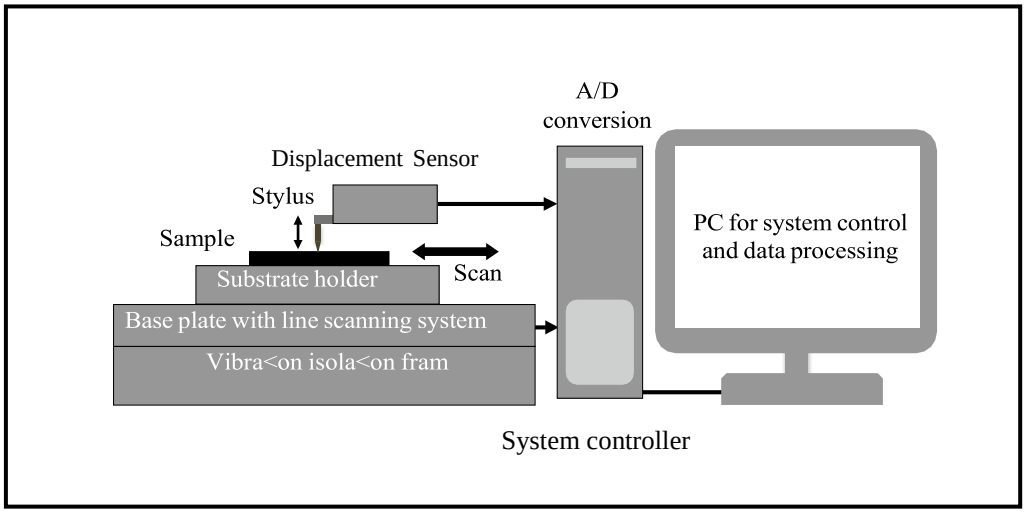

Fig.II.13 – Diagram of a surface profilometer [36] .

In this work, the thickness of the prepared thin films was measured using KLA Tencor surface profilometer.

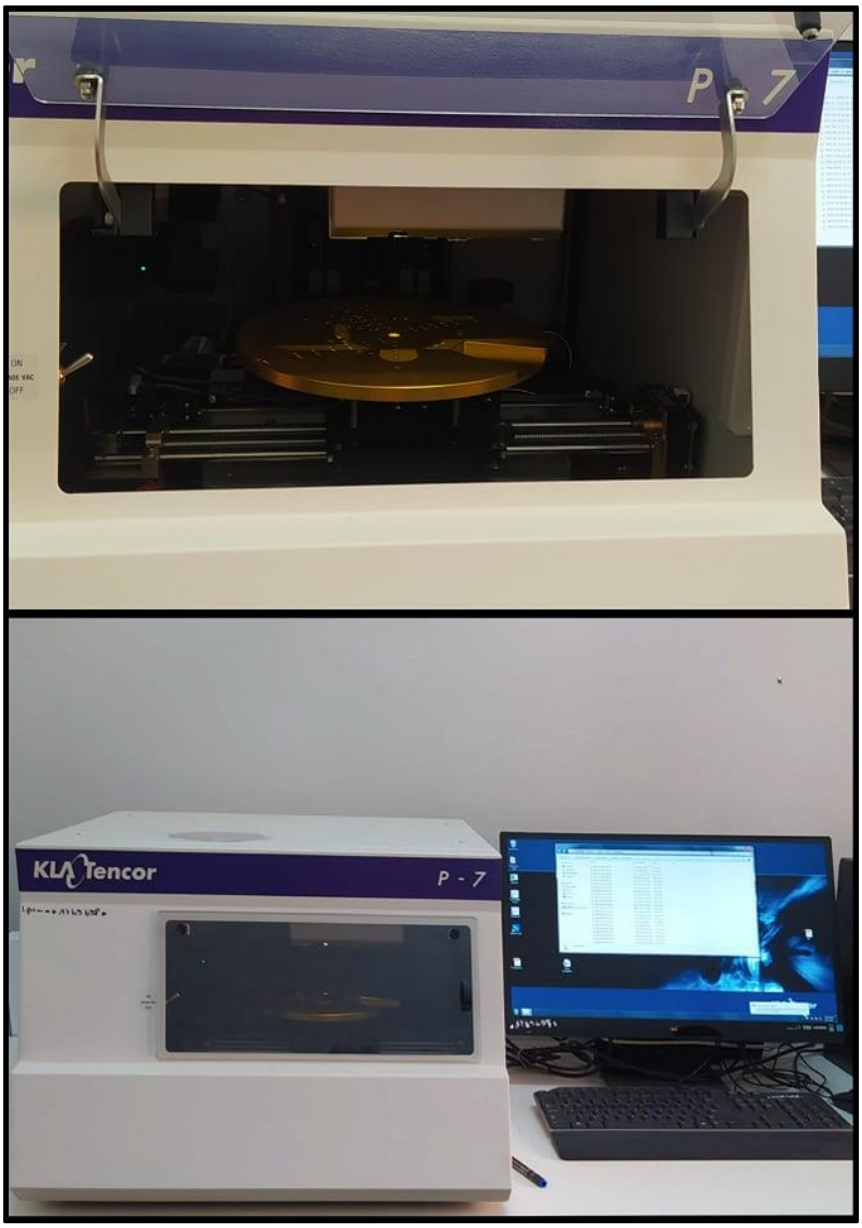

Fig.II.14 – Surface profilometer.

Chapter 3

Results and Discussion

This chapter is devoted to analysis the deposited thin films using the characterization methods mentioned in the previous chapter (chapter2) in the laboratory (LPCMA) of the University of Biskra . Through this study we can know the general properties of the titanium dioxide such as structural, optical and morphological properties and the influence of Cu doping on these properties.

III – 1 – Morphological characterization :

The surface morphology of the pure TiO_2 and Cu doped TiO_2 thin films before and after annealing were characterized using TESCAN VEGA 3 scanning electron microscope.

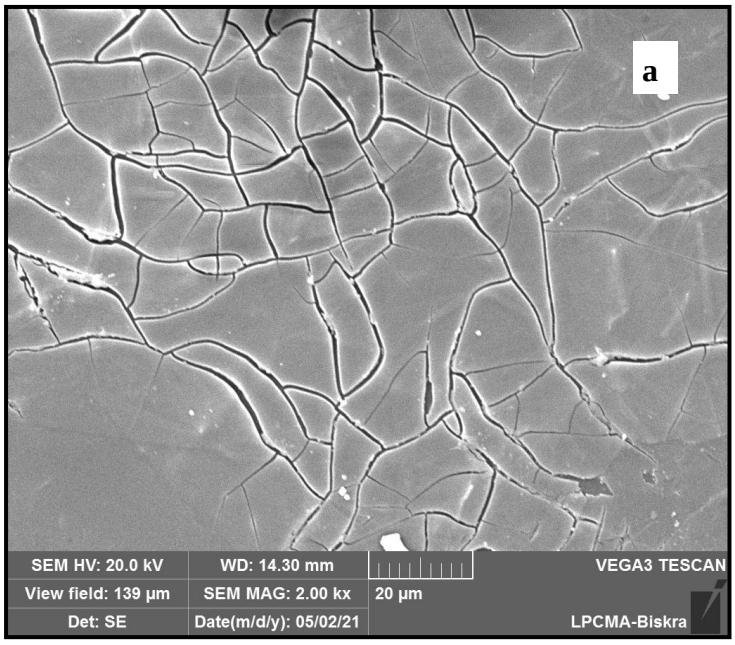

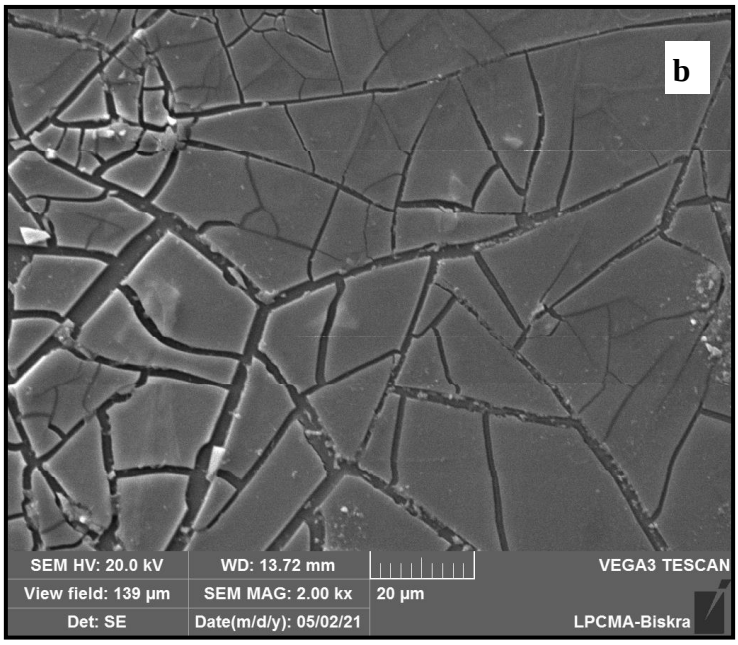

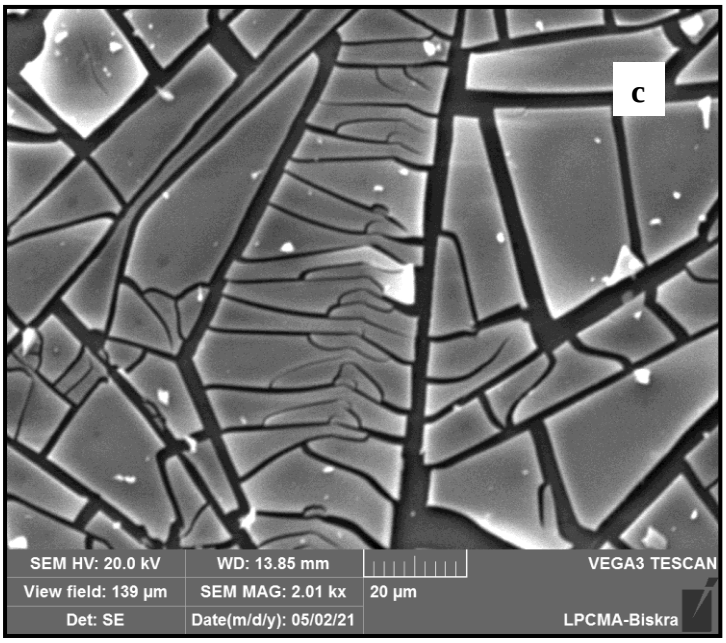

Fig.III.1 – SEM Images of Cu doped TiO_2 thin films with different Cu concentrations (a) : $3{,}404x10^{-5}$mol/l , (b) :$1{,}702x10^{-5}$mol/l , (c) : $8{,}511x10^{-6}$mol/l .

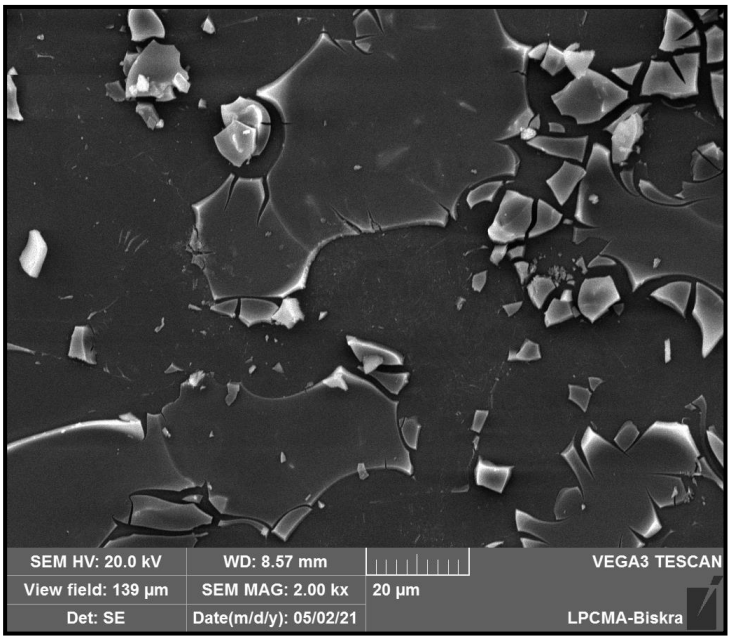

Fig.III.2–SEM Image of pure TiO_2thin film before annealing

- The SEM images illustrates a few localized agglomerations in the surface of the films with cracked patterns .The crack formation was possibly by the repeated process done to make thicker coatings of films (5 layers) [37].

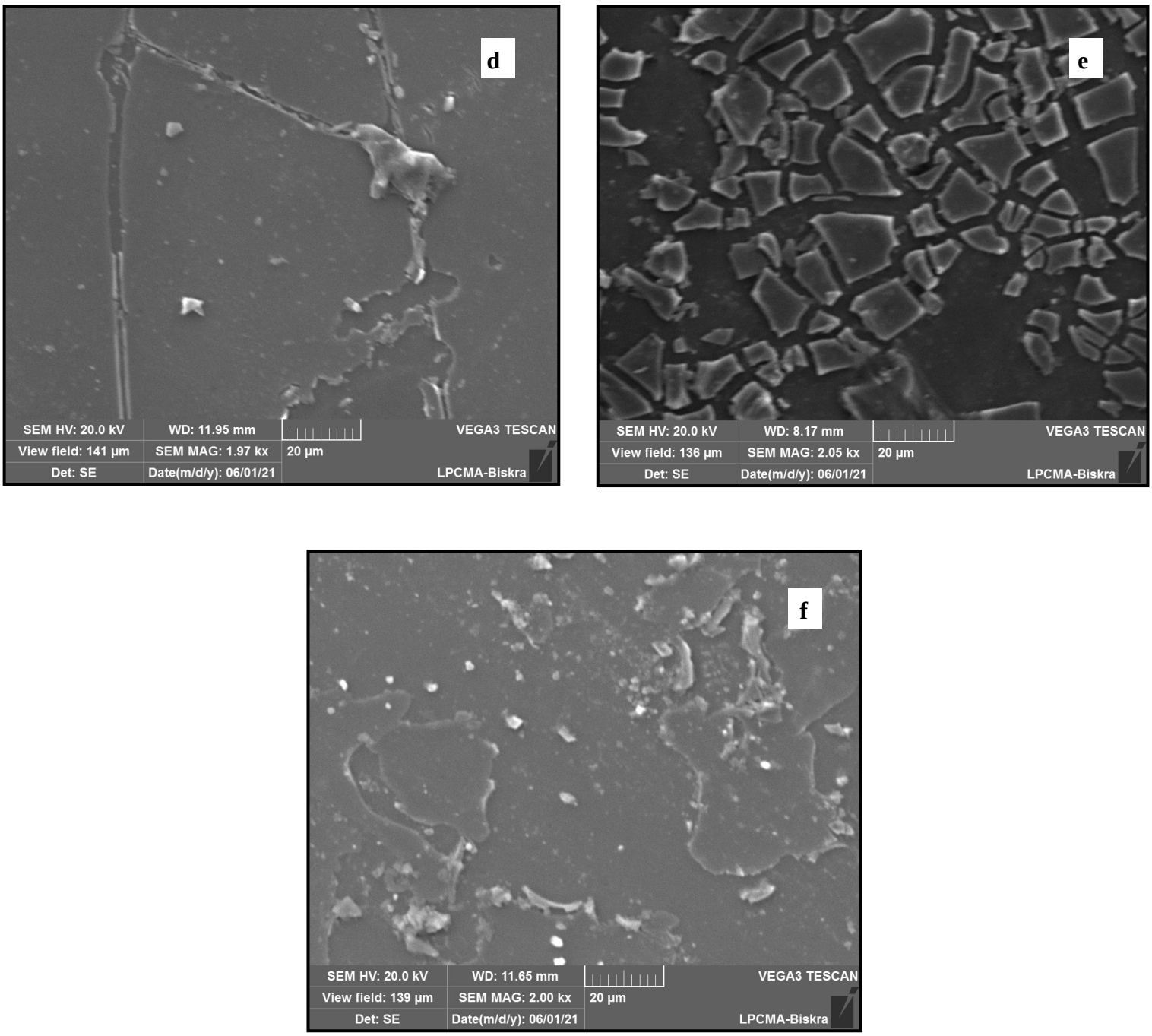

Fig.III.3 – SEM Images of Cu doped TiO2 thin films with different Cu concentrations after annealing: (d) : 3,404x10^{-5}mol/l, (e) : 1,702x10^{-5}mol/l, (f) : 8,511x10^{-6}mol/l .

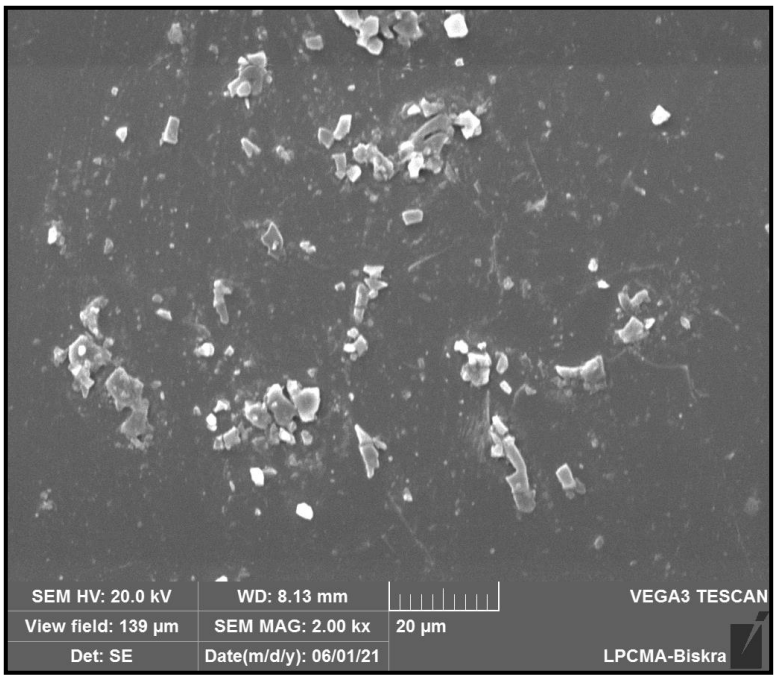

Fig.III.4 –SEM Image of pure TiO_2 thin film after annealing.

-Fig.III.3 (a), (b) and fig.III.4 shows loosely agglomerated, irregular smaller grains with flake like morphology [38].

- Fig.III.3 (e) shows loosely agglomerated grains with mosaic like structure. The dipping process was repeated five times to make the coatings thicker. In this case small cracks, pin holes and island like structures form when the film thickness is increased [39].

III – 2 – Energy dispersive X-ray spectroscopy (EDX) characterization:

Energy dispersive X-ray spectroscopy was used to determine the chemical composition of the pure $TiO_2$and Cu-TiO_2 thin films, the EDX spectrums of the elaborated films are shown in fig.III.5 and fig.III.6 before and after annealing.

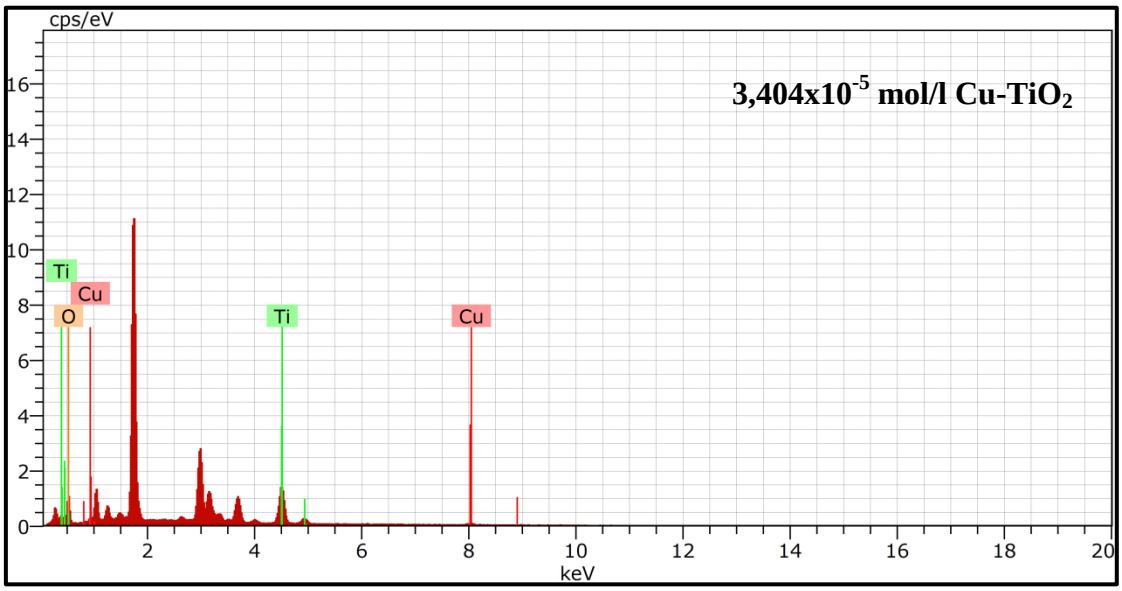

ElANSeriesunn.C	norm.C [wt.%]	Atom.C [wt.%]	Error(1 Sigma) [wt.%]
O8K-series	9.80	59.96	82.15	1.61
Ti22K-series	5.85	35.79	16.39	0.20
Cu29K-series	0.69	4.25	1.47	0.06
Total:	16.34	100.00	100.00	

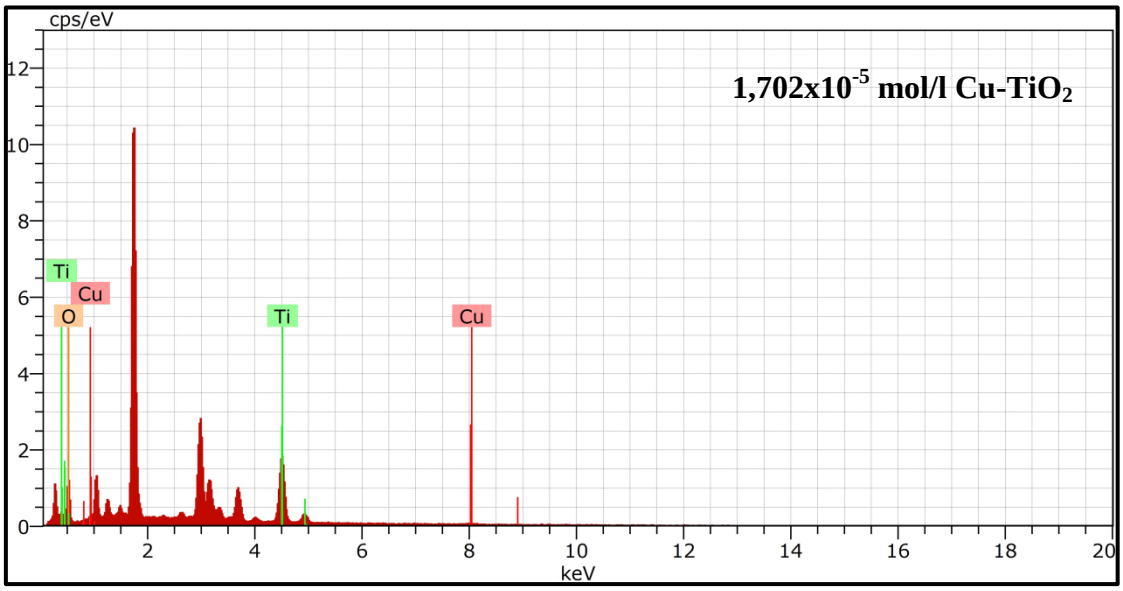

ElANSeriesunn.C	norm.C [wt.%]	Atom.C [wt.%]	Error(1 Sigma) [wt.%]
O8K-series	11.59	60.34	82.22	1.86
Ti22K-series	7.16	37.24	16.96	0.23
Cu29K-series	0.46	2.42	0.83	0.05
Total:	19.21	100.00	100.00	

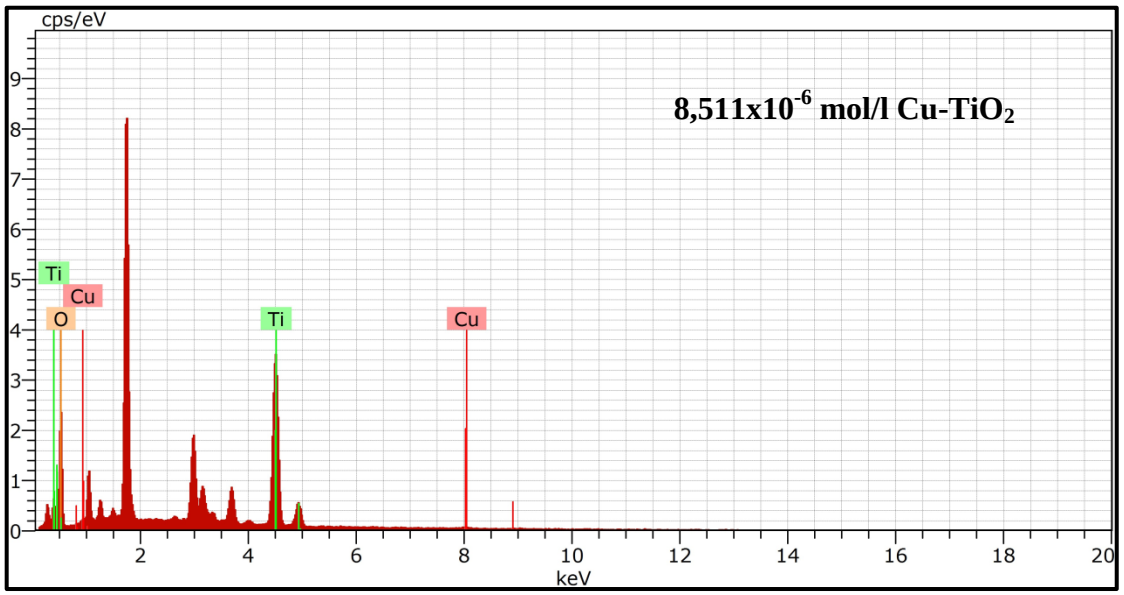

ElANSeriesunn.C	norm.C [wt.%]	Atom.C [wt.%]	Error(1 Sigma) [wt.%]
O8K-series	25.21	61.07	82.53	3.55
Ti22K-series	15.64	37.89	17.11	0.47
Cu29K-series	0.43	1.04	0.36	0.05
Total:	41.27	100.00	100.00	

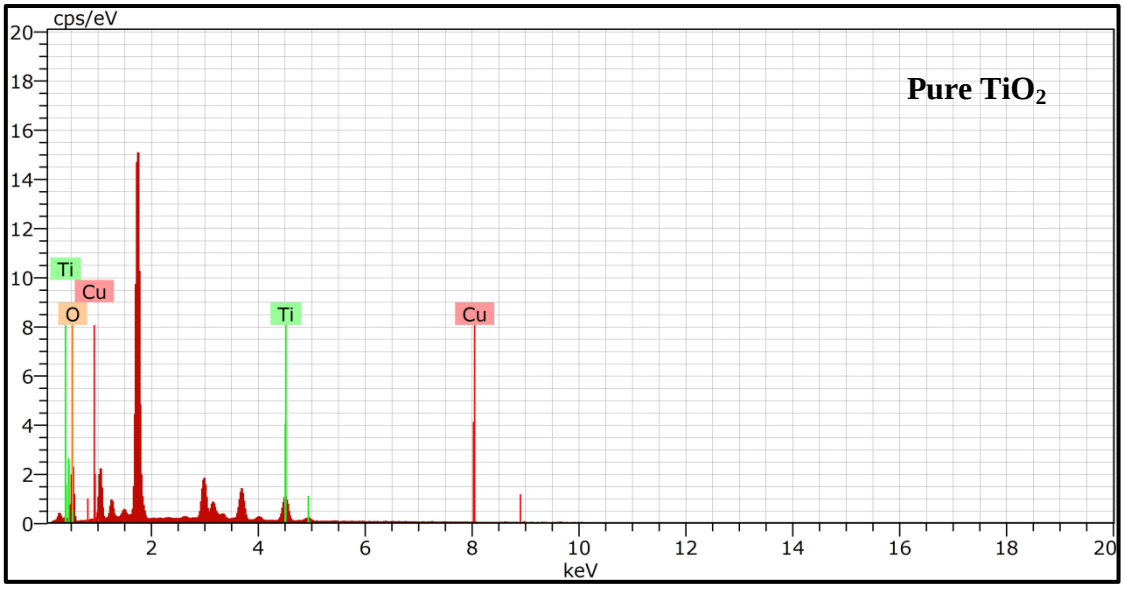

ElANSeriesunn.C	norm.C [wt.%]	Atom.C [wt.%]	Error(1 Sigma) [wt.%]
O8K-series	15.74	77.27	91.06	2.27
Ti22K-series	4.60	22.60	8.90	0.16
Cu29K-series	0.03	0.13	0.04	0.03
Total:	20.36	100.00	100.00	

Fig.III.5 –EDX spectrums of pure TiO_2 and Cu-TiO_2 thin films with different Cu concentrations before annealing

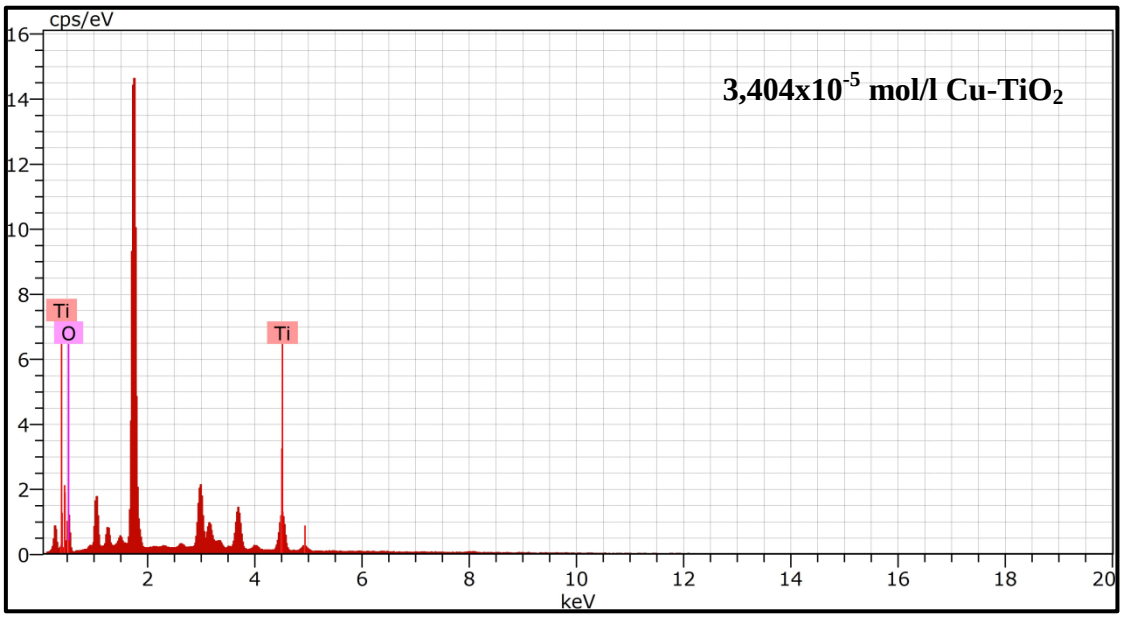

ElANSeriesunn.C	norm.C [wt.%]	Atom.C [wt.%]	Error(1 Sigma) [wt.%]
O8K-series	8.92	67.83	86.32	1.46
Ti22K-series	4.23	32.17	13.68	0.15
Total:	13.14	100.00	100.00	

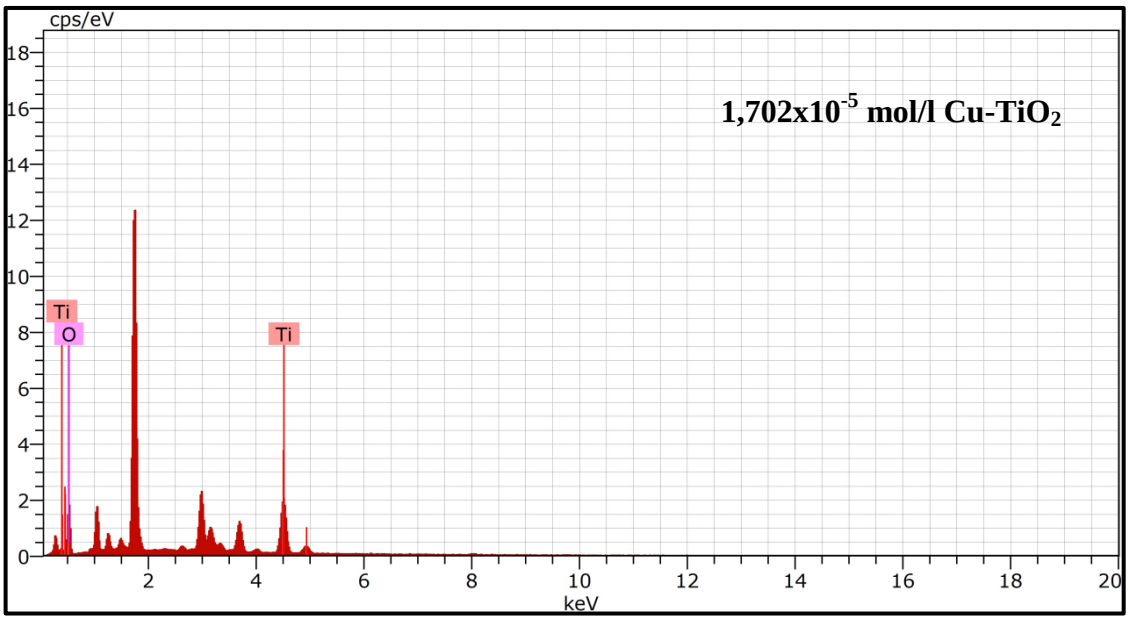

ElANSeriesunn.C	norm.C [wt.%]	Atom.C [wt.%]	Error(1 Sigma) [wt.%]
O8K-series	14.51	66.70	85.70	2.18
Ti22K-series	7.25	33.30	14.30	0.23
Total:	21.76	100.00	100.00	

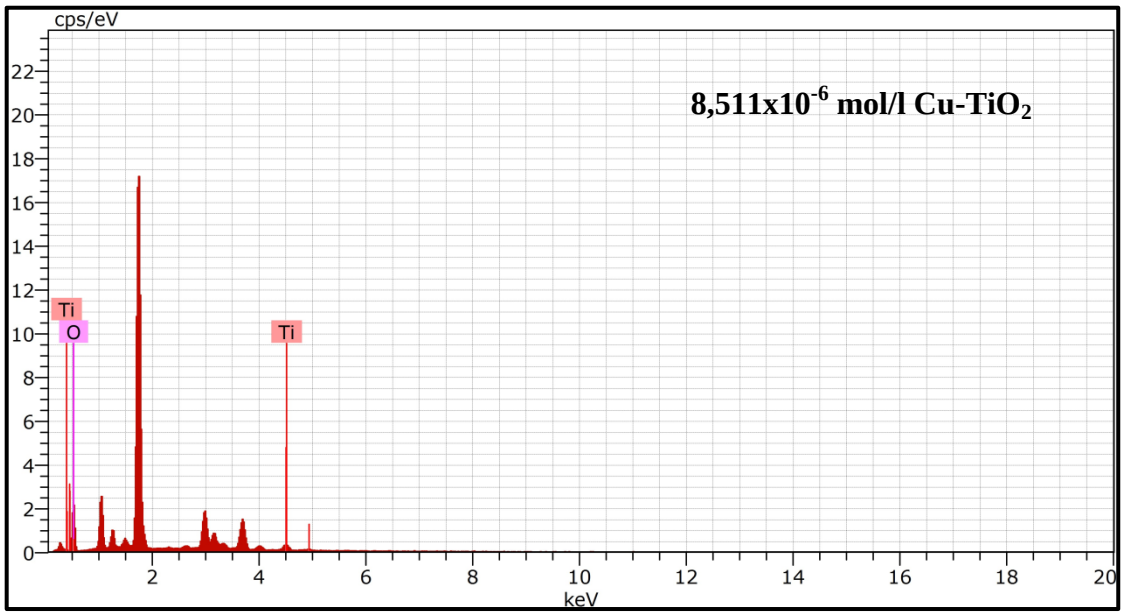

ElANSeriesunn.C	norm.C [wt.%]	Atom.C [wt.%]	Error(1 Sigma) [wt.%]
O8K-series	91.29	96.91	13.29
Ti22K-series	8.71	3.09	0.37
Total:	100.00	100.00	

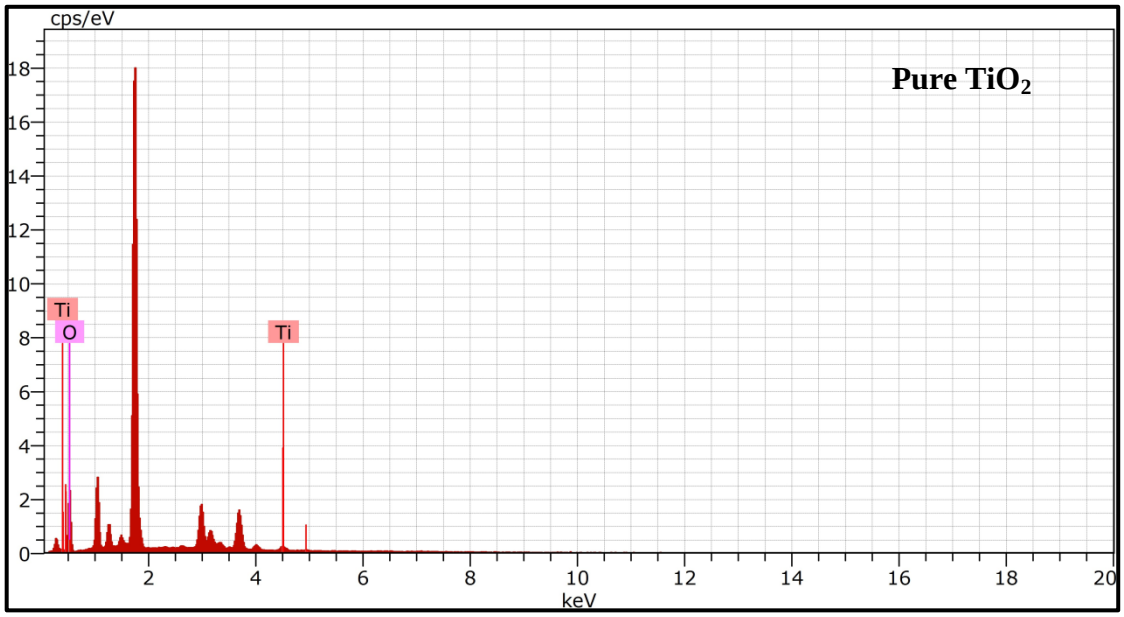

ElANSeriesunn.C	norm.C [wt.%]	Atom.C [wt.%]	Error(1 Sigma) [wt.%]
O8K-series	7.11	88.73	95.93	1.06
Ti22K-series	0.90	11.27	4.07	0.06
Total:	8.01	100.00	100.00	

Fig.III.6–EDX spectrums of pure TiO_2 and Cu-TiO_2 thin films with different Cu concentrations after annealing

-The EDX spectrums before annealing expose the presence of titanium, copper and oxygen in the prepared thin films in dissimilar proportions.

- The absence of copper in the EDX spectrums after annealing is due to the existence of copper with low proportions in the films, and this technique can't detect it.

III – 3 – Structural characterization:

The XRD diffractograms of pure TiO_2 and Cu doped TiO_2 thin films before and after annealing are shown in fig.III.7 and fig.III.8.

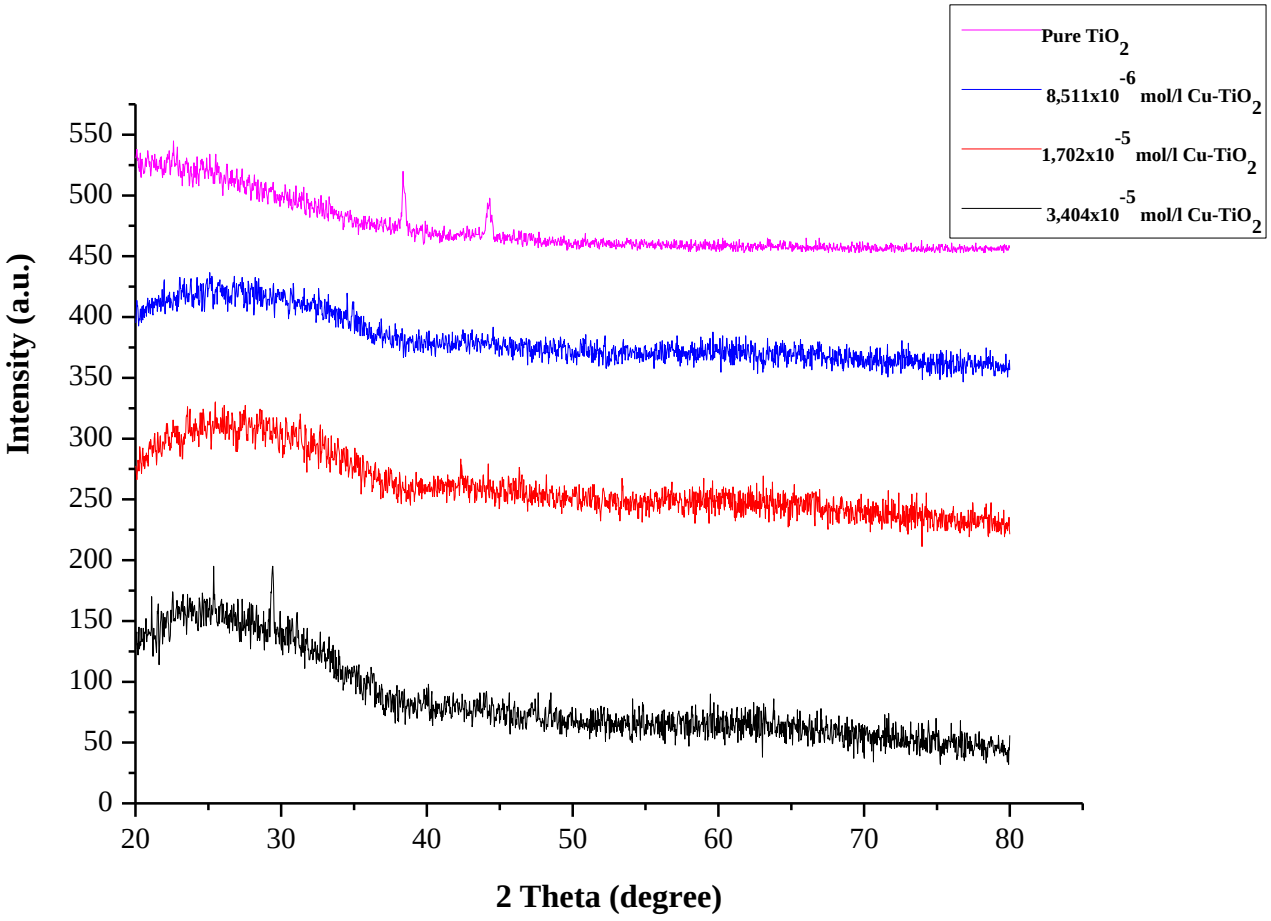

Fig.III.7 –XRD patterns of pure TiO_2 and Cu-TiO_2 thin films with different Cu concentrations before annealing

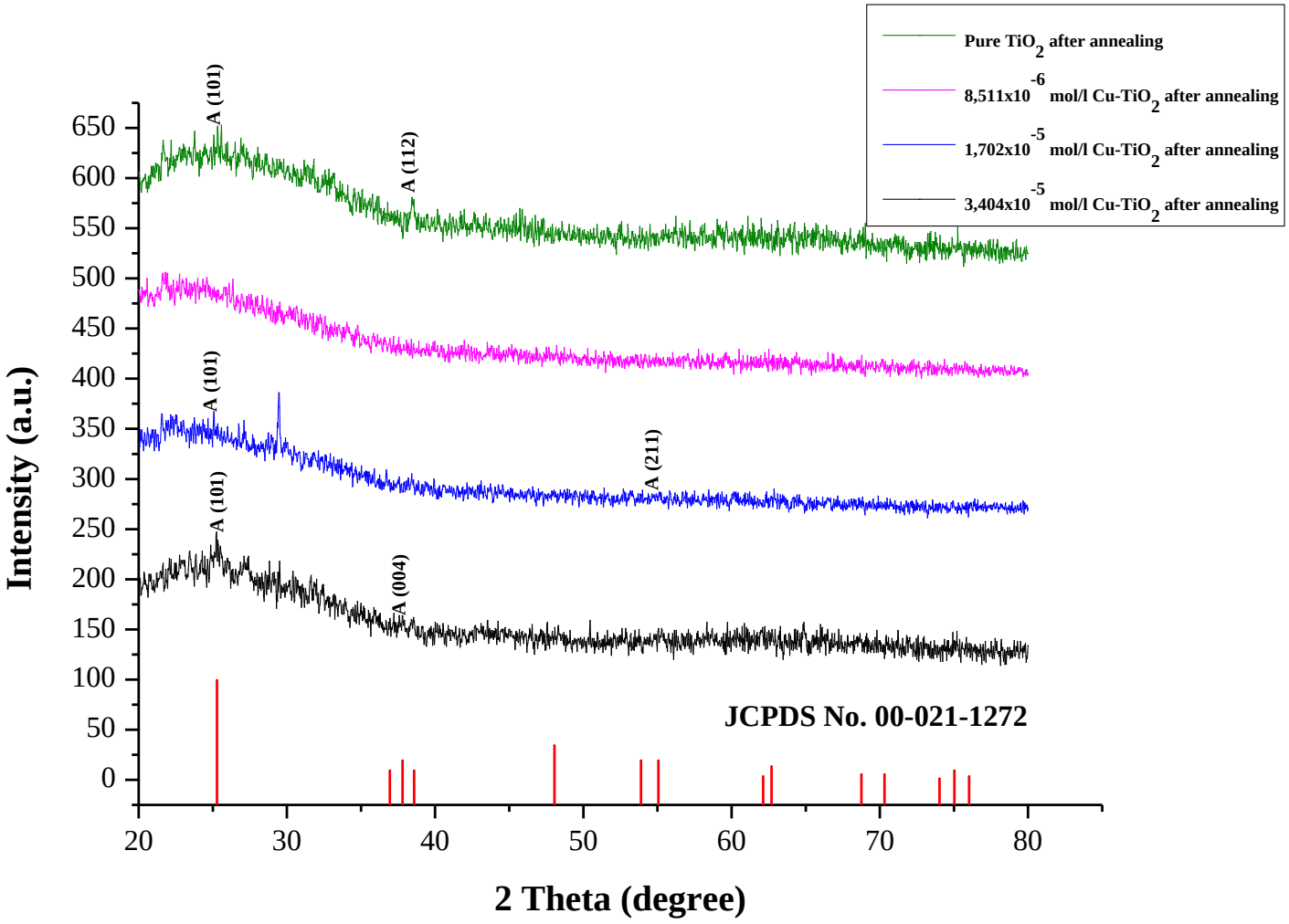

Fig.III.8–XRD patterns of pure TiO_2 and Cu-TiO_2 thin films with different Cu concentrations after annealing at 400 °C

From the XRD pattern, it is observed that the prepared thin films before annealing were amorphous. While after annealing both pure TiO_2 and Cu doped TiO_2 thin films show a tetragonal crystal structure of anatase phase with preferential orientation along (101) plane which is in agreement with JCPDS file no 21-1272. However, no peaks related to Cu impurities are found due to the low doping concentrations of Cu or the Cu metal ions have been well dispersed into the TiO_2 matrix in the form of small cluster [37].

III – 4 – Thickness measurement:

The thickness of pure TiO_2 and Cu doped TiO_2 thin films were measured using KLA Tencor surface profilometer. Thickness values are shown in the table below :

Table.III.1 – Thickness values of pure TiO_2 and Cu-TiO_2 thin films before and after annealing at 400 °C

Cu concentration (mol/l)	Thickness before annealing (µm)	Thickness after annealing at 400 °C(µm)
0	0,50706	0,45321
$8{,}511x10^{-6}$	0,24598	0,55545
$1{,}702x10^{-5}$	1,189	0,09672
$3{,}404x10^{-5}$	0,63327	0,66647

III – 5 – Optical characterization:

III – 5 – 1 –Transmittance spectrums:

Transmittance spectrums of pure TiO_2 and Cu doped TiO_2 thin films before and after annealing were measured using JASCO UV-Visible spectrophotometer , the spectrums are illustrated in fig.III.9 and fig.III.10 .

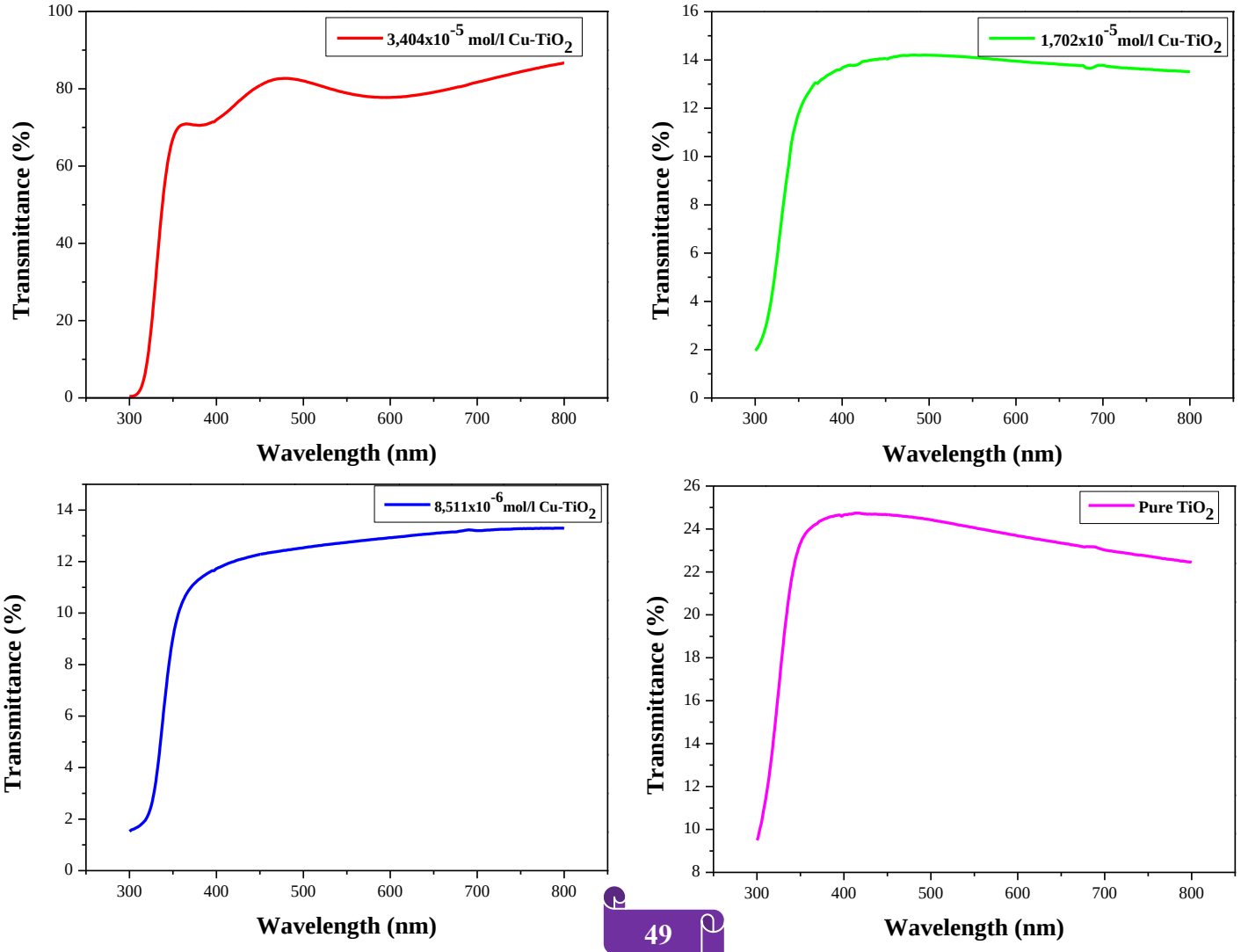

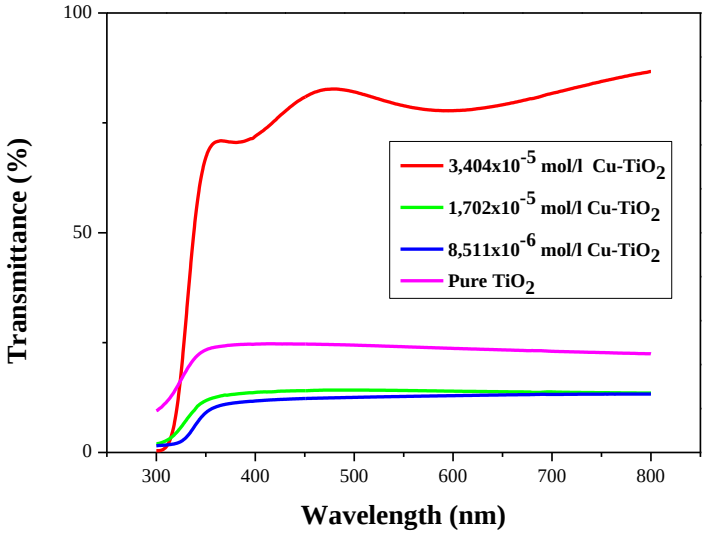

Fig.III.9 – Transmittance spectrums of pure TiO_2 and Cu-TiO_2 thin films before annealing

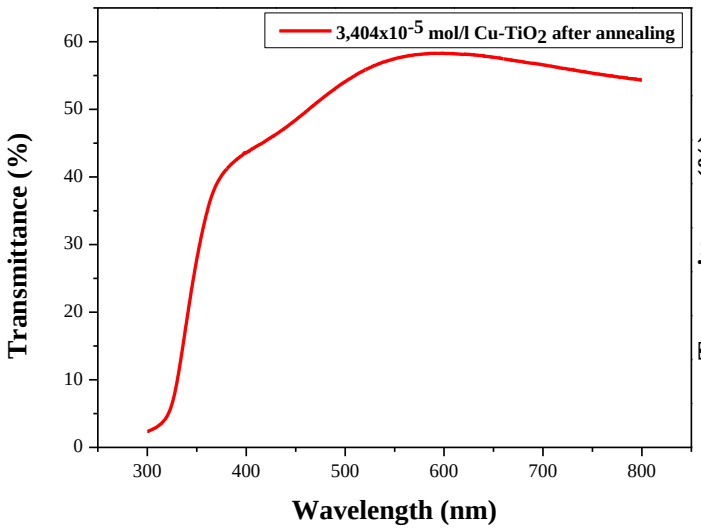

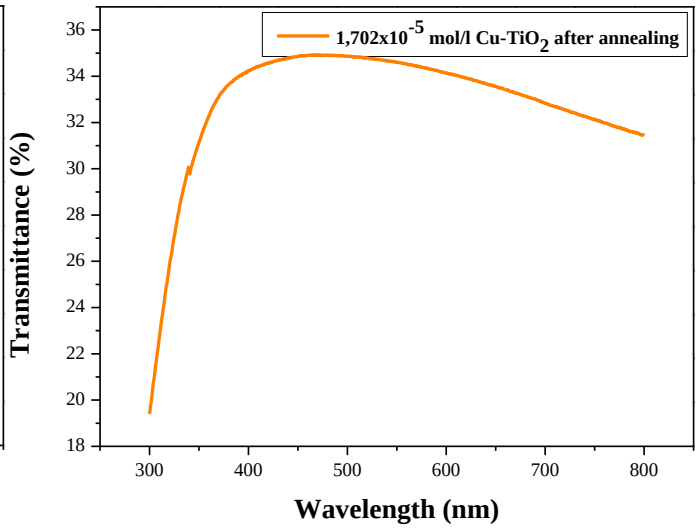

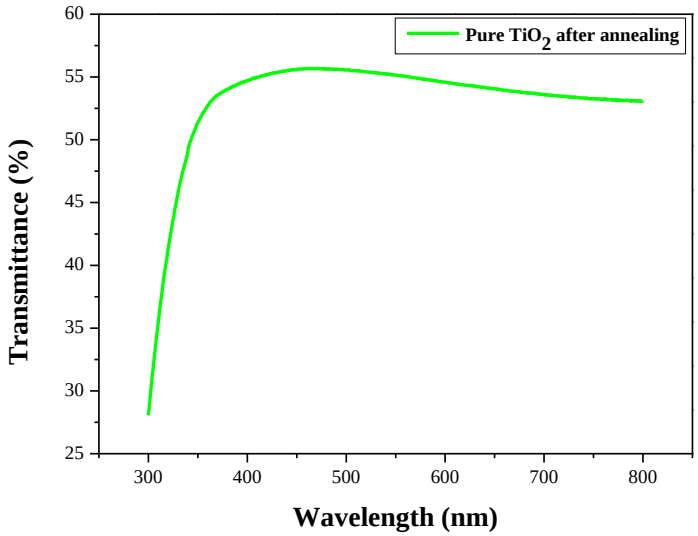

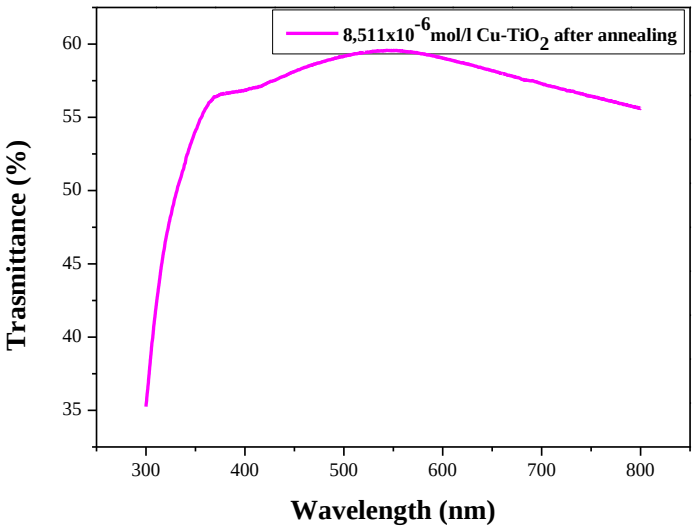

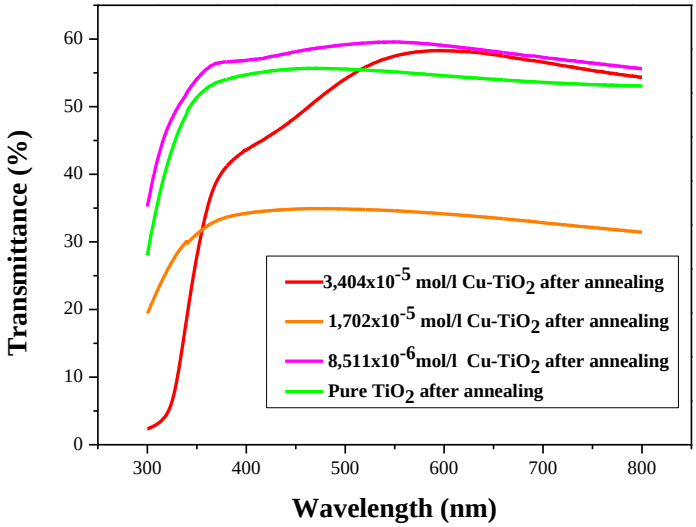

Fig.III.10 – Transmittance spectrums of pure TiO_2 and Cu-TiO_2 thin films after annealing

From the transmittance spectrums, it is observed that:

- The transmittance begins to fall off at a wavelength of about 380 nm. The decrease in transmittance is due to the absorption of light that had caused the excited electron to immigrate from valence band to the conduction band [31] .

- the highest transmittance value of Cu-TiO_2 film with concentration of 3,404x10^{-5}mol/l before annealing where about 80 %, this value decrease to 58 % after annealing at 400 °C, this decrease in the transmittance can be related to the increased scattering of photons by crystal defects by doping [40] .

- For the rest of the samples the transmittance before annealing varies between 13 -25% in the visible region.

- The values of transmittance of both pure $TiO_2$and Cu-$TiO_2$with lower Cu concentrations films increase after annealing which could be attributed to the differences in the nature of microstructure, thicknesses and surface morphology of the TiO2 films[41].

III – 5 – 2 – Band gap energy :

The direct and indirect energy band gap of the pure TiO_2 and Cu-TiO_2 thin films before and after annealing was calculated by the method explained in the previous chapter and are shown in fig.III.11,fig.III.12, fig.III.13 and fig.III.14 .

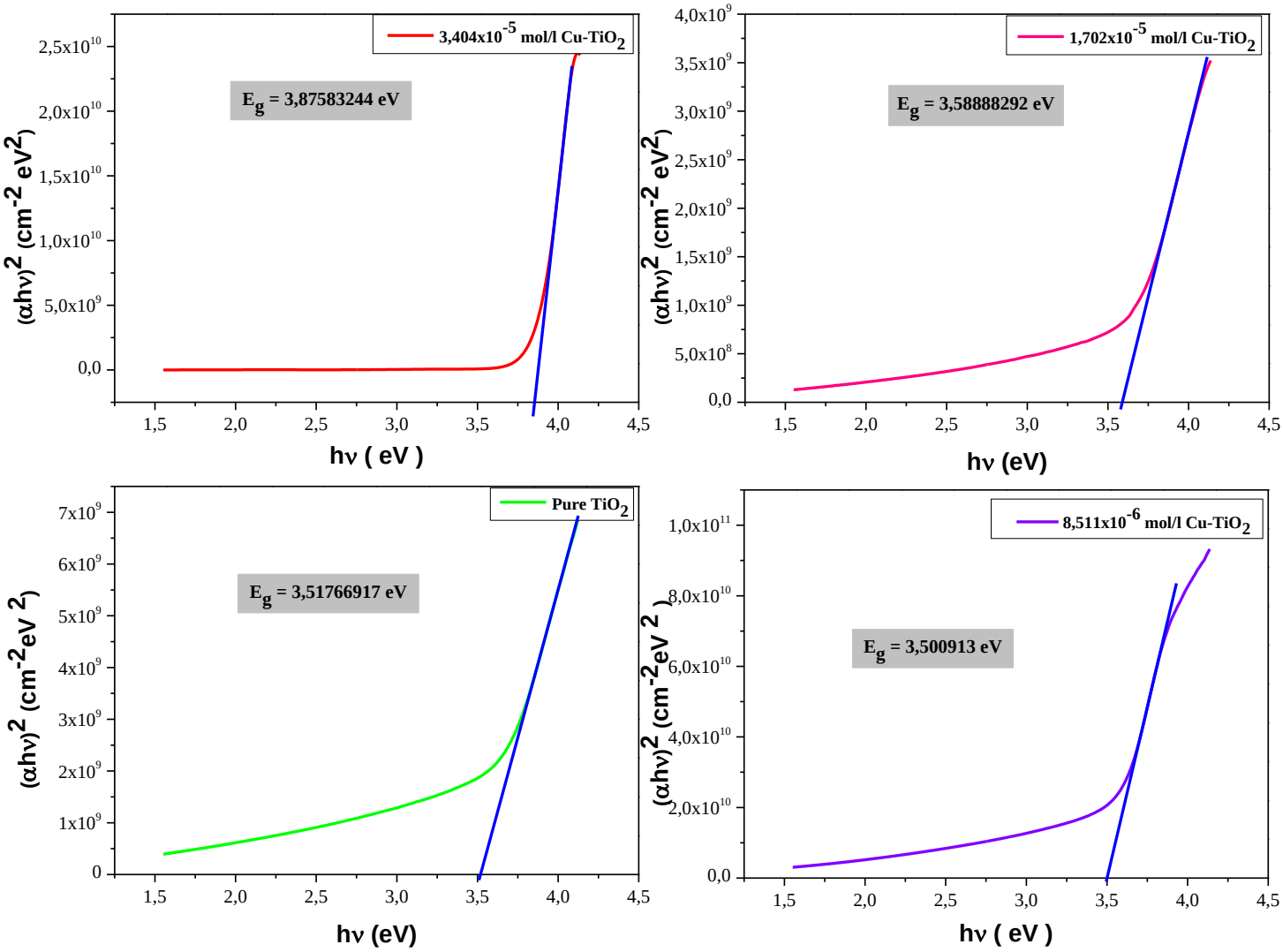

Fig.III.11 – Direct band gap of pure TiO_2 and Cu-TiO_2 thin films before annealing

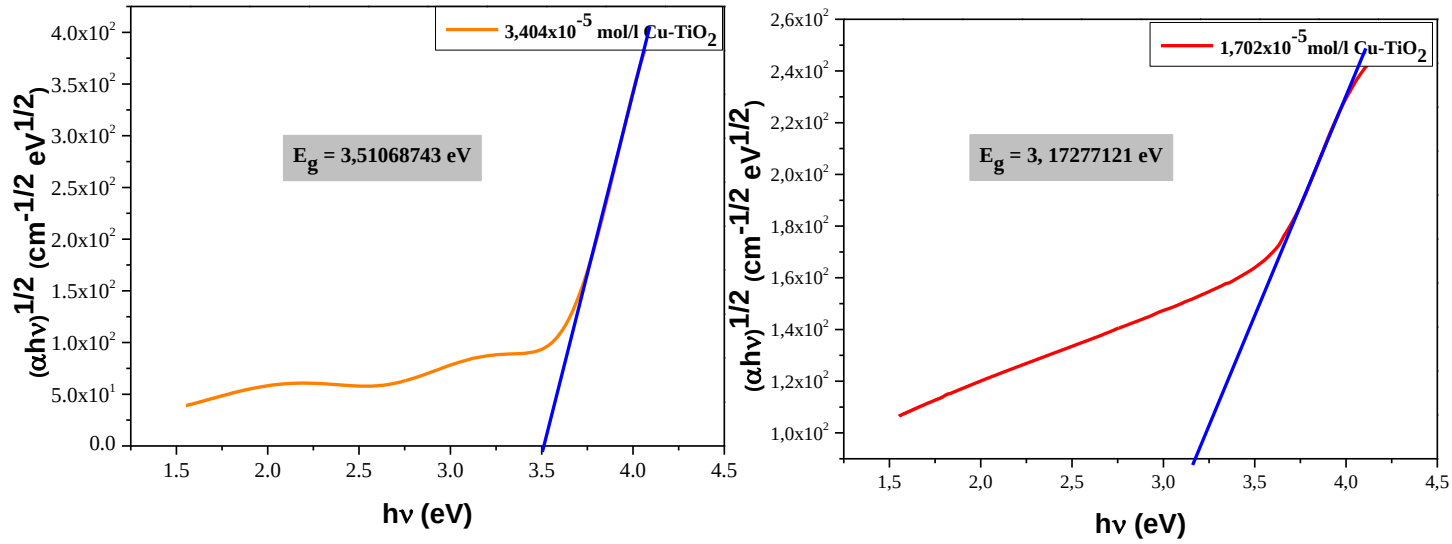

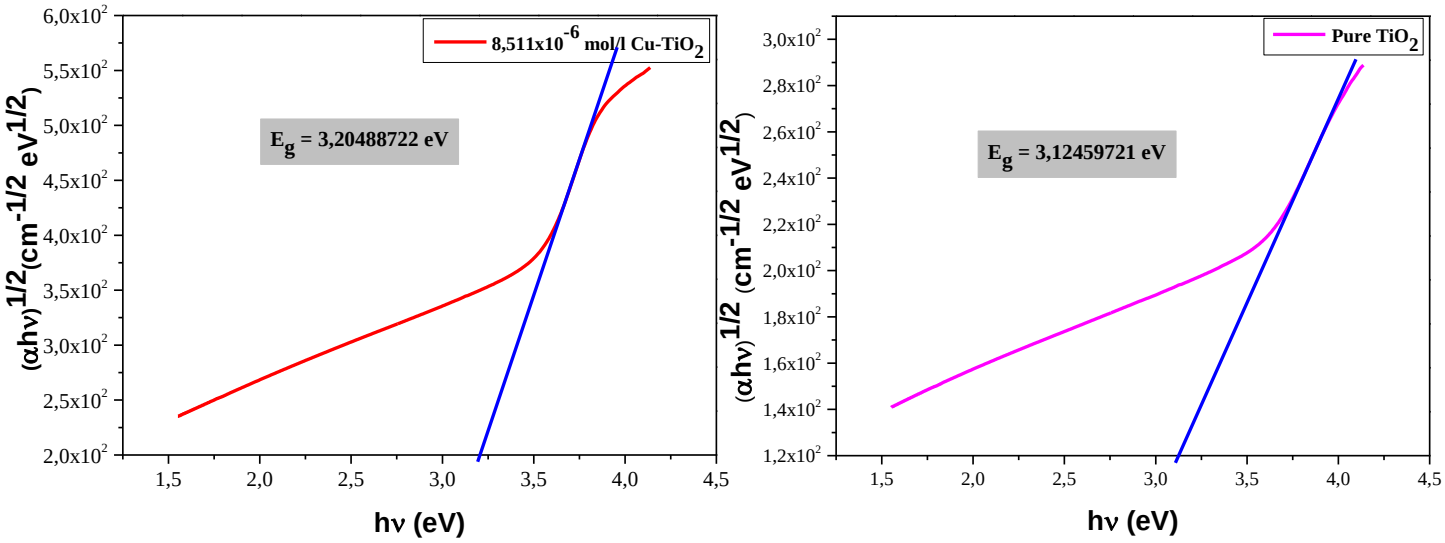

Fig.III.12 – Indirect band gap of pure TiO_2 and Cu-TiO_2 thin films before annealing

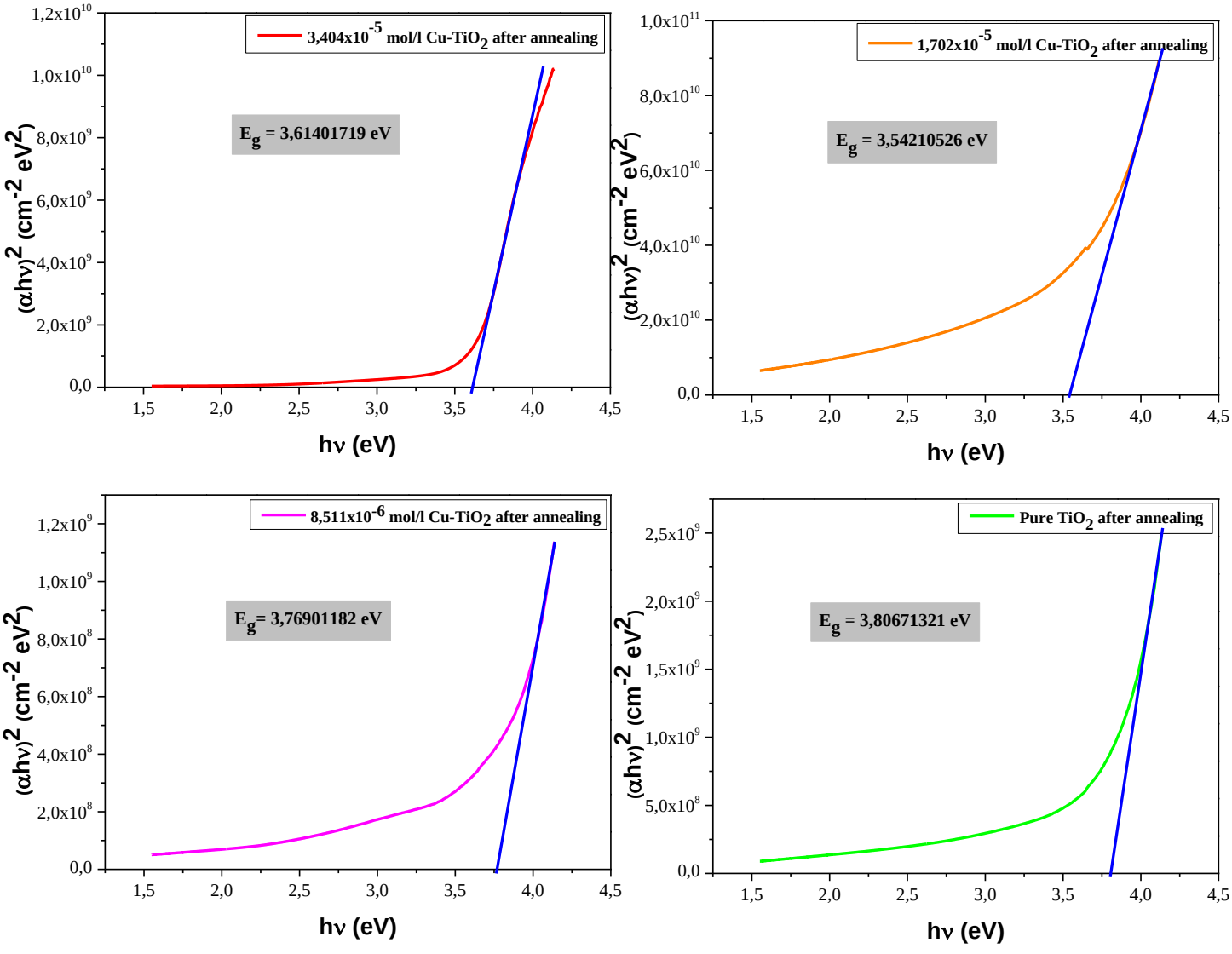

Fig.III.13 – Direct band gap of pure TiO_2 and Cu-TiO_2 thin films after annealing

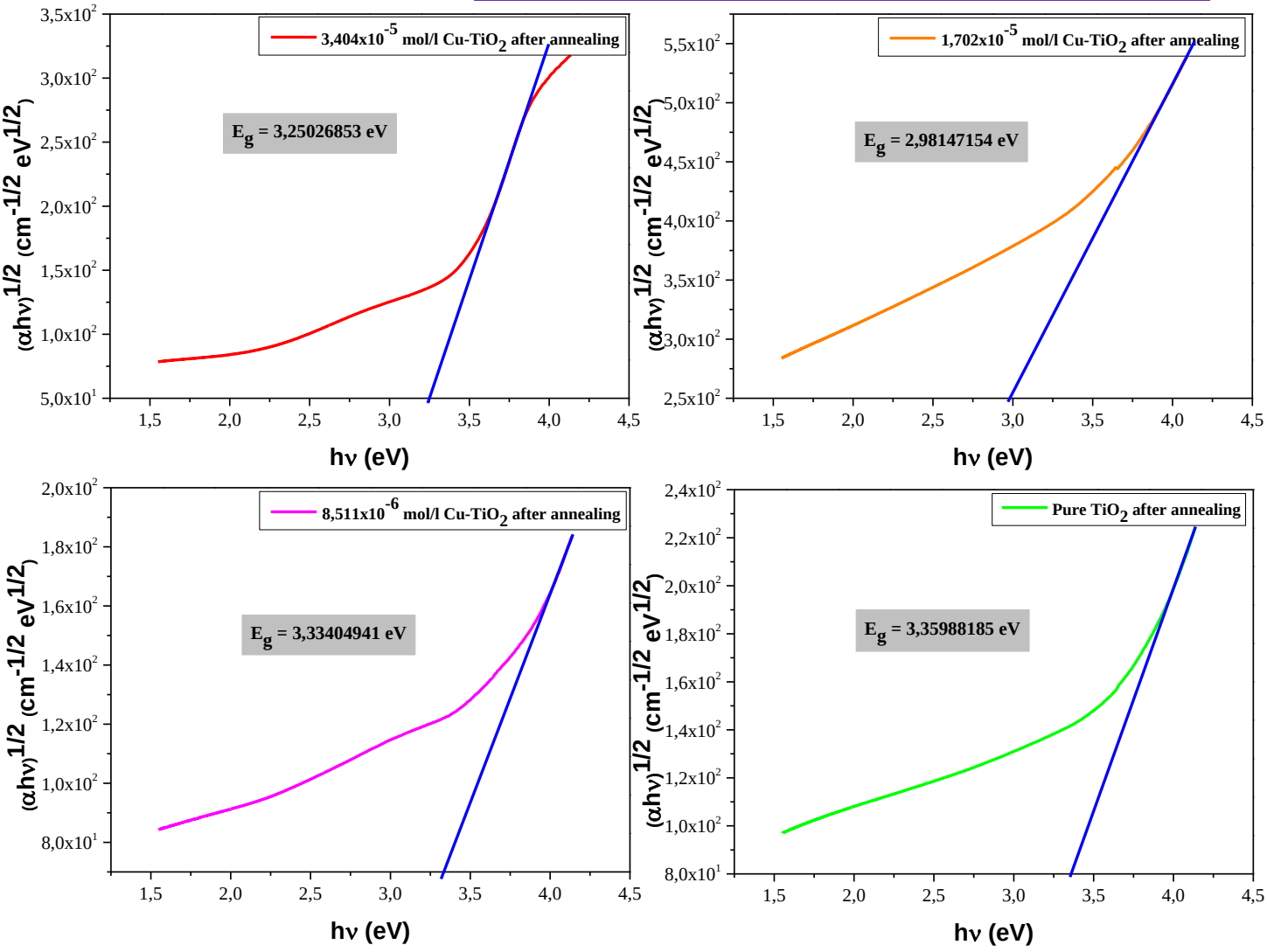

Fig.III.14 – Indirect band gap of pure TiO_2 and Cu-TiO_2 thin films after annealing

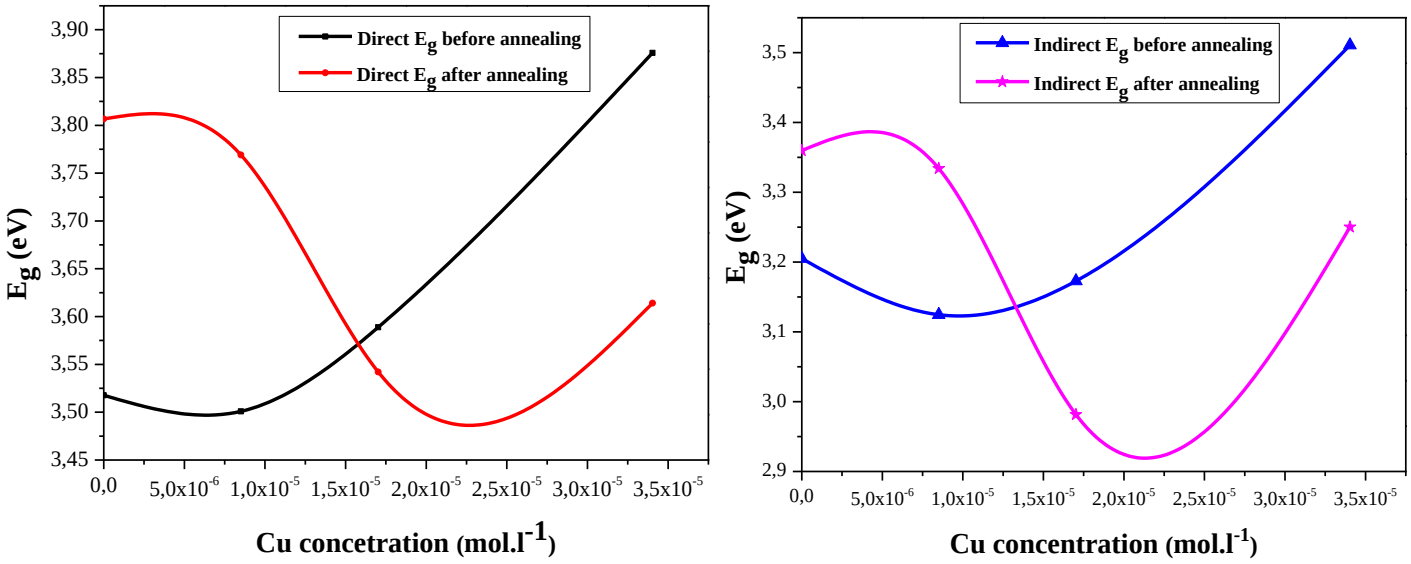

Fig.III.15 –The variation of the optical band gap direct and indirect of the prepared films before and after annealing at 400 °C in function of the Cu concentration .

Table.III.1 – The variation of the optical band gap direct and indirect of the prepared films before and after annealing with the Cu concentration.

Cu concentration (mol/l)	Optical band gaps E_g before annealing (eV)		Optical band gaps E_g after annealing (eV)	
	Direct gap	Indirect gap	Direct gap	Indirect gap
0	3,51766917	3,12459721	3,80671321	3,35988185
$8{,}511x10^{-6}$	3,500913	3,20488722	3,76901182	3,33404941
$1{,}702x10^{-5}$	3,58888292	3,17277121	3,54210526	2,98147154
$3{,}404x10^{-5}$	3,87583244	3,51068743	3,61401719	3,25026853

Fig. III.15 shows that there is a decrease in the energy of the direct and indirect band gap after annealing compared with the energy band gap of pure TiO_2 film. These variations can be explained by the Cu doping creates new electronic levels and reduces the band gap energy [37].

General Conclusion

Our study is concerned about elaboration and characterization of undoped and copper doped titanium dioxide thin films deposited by sol-gel dip coating method in order to investigate the effect of doping on the structural, morphological and optical properties of the prepared thin films. For that, we carried out a series of samples on glass substrates by the sol-gel dip coating method, and then we annealed the samples at 400 °C for 3 hours, for better crystallinity.

- The morphological characterization by SEM shows that:
  - The surface of the prepared films before annealing has a few localized agglomerations with cracked patterns.
  - The surfaces of the prepared films (except the $1{,}702 \times 10^{-5}$ mol/l Cu-TiO_2 film) after annealing were loosely agglomerated, irregular smaller grains with flake like morphology.
  - The surface of the film with Cu concentration of $1{,}702 \times 10^{-5}$ mol/l after annealing was loosely agglomerated grains with mosaic like structure.
- The characterization of chemical composition by EDX spectroscopy shows that:
  - The EDX spectrums before annealing expose the presence of titanium, copper and oxygen in the prepared thin films in dissimilar proportions.
  - The absence of copper in the EDX spectrums after annealing is due to the existence of copper with low proportions in the films, and it can't be detected.
- The structural characterization by DRX shows that :
  - The pure TiO_2 and Cu doped TiO_2 thin films before annealing were amorphous, after annealing the films show a tetragonal crystal structure of anatase phase with preferential orientation along (101) plane.
- Thickness of the pure TiO_2 and Cu-TiO_2 thin films :
  - The thickness of the prepared films was in the range of 1,189-0,096 μm.
- Optical characterization by UV-Visible spectroscopy shows that:

- The highest transmittance value of Cu-TiO_2 film with concentration of $3{,}404 \times 10^{-5}$ mol/l before annealing where about 80 %, this value decrease to 58 % after annealing at 400 °C.
- For the rest of the samples the transmittance before annealing varies between 13 -25 % in the visible region.
- The values of transmittance of both pure TiO_2 and Cu-TiO_2 with lower Cu concentrations films increase after annealing.
- The energy of the direct and indirect band gap of the pure TiO_2 and Cu- TiO_2 thin films in the range of 3,8 - 2,9 eV .
- The energy of the direct and indirect band gap of the Cu- TiO_2 thin films decrease after annealing compared with the energy band gap (direct and indirect) of pure TiO_2 film .

Perspectives:

To improve the optical properties of TiO_2 thin films to make them efficient in photocatalytic and photovoltaic applications, we suggest:

- Modify the experimental conditions used and the copper doping concentration.
- Using non-metal doping such as carbon doped TiO_2.
- Using co-doping.

References

[1] M. Endresen Alnes, Transparent Conducting Oxides by Atomic Layer Deposition, Ph.D Thesis, University of Oslo, Norway (2014).

[2] H. ARSLAN, Indium Tin Oxide (ITO) Coating on Cylindrical Surfaces: Electrical and Structural Characterization, Master Thesis, Izmir Institute of Technology, Turkey (2015).

[3] T.V. Vimalkumar, Highly conductive and transparent ZnO thin film using Chemical Spray Pyrolysis technique: Effect of doping and deposition parameters Ph.D thesis, Cochin University of Science and Technology, India (2011).

[4] R. A. Afre, N. Sharma, Mh. Sharon and Md. Sharon, Transparent Conducting Oxide Films for Various Applications: A Review, Rev. Adv. Mater. Sci, 53, (2018), 79-89.

[5] A. J. Haider a, Z. N. Jameel, I. H. M. Al-Hussaini, Review on: Titanium Dioxide Applications, Energy Procedia, 157, (2019), 17-29.

[6] J. Y Ruzicka, Synthesis of titanium dioxide nanoparticles: phase, morphology and size control, Ph.D Thesis, University of Canterbury, New Zeland (2013).

[7] A. Nakaruk, Synthesis and Characterisation of Titania Thin Films, Ph.D thesis, University of New South Wales, (2010).

[8] S. Sarcar, Synthesis and study of cation doped Titanium dioxide nanoparticles, Master thesis, Amity University, India (2014).

[9] M. Dahnoun, Preparation and characterization of Titanium dioxide and Zinc oxide thin films via Sol-Gel (spin coating) technique for optoelectronic applications, PhD thesis, University Mohamed Khider of Biskra, (2020).

[10] G. Raza, Titanium Dioxide Nanomaterials, Synthesis, Stability and Mobility in Natural and Synthetic Porous Media, Ph.D thesis, The University of Birmingham, England (2016).

[11] A. E. Shalan, A. M. Elseman and M. M. Rashad, Titanium Dioxide - Material for a Sustainable Environment, Intech Open, (2018), 353-354.

[12] R. MESSEMCHE, Elaboration and characterization of undoped and doped titanium dioxide thin layers by sol gel (spin coating) for photocatalytic applications, Ph.D thesis, University Mohamed Khider of Biskra, (2021).

[13] M. Kwiatkowski, ZnO (core)/TiO_2 (shell) composites: influence of TiO_2 microstructure, N-doping and decoration with Au nanoparticles on photocatalytic and

photoelectrochemical activity, Ph.D thesis, University Bourgogne Franche-Comté, France (2017).

[14] R. A. Buky, Tunning Functionality of Photocatalytic Materials: an Infrared Study on Hydrocarbon Oxidation, Ph.D thesis, University of Twente, Pays Bas (2016).

[15] P A J Lusty, S D Hannism, Commodity Profile: Copper, British Geological Survey, Internel Report OR/09/041, (2009).

[16] A. Nakaruk, Synthesis and Characterisation of Titania Thin Films, Ph.D thesis, University of New South Wales, (2010).

[17] A. Zhao, Optical Properties, Electronic Structures and High Pressure Study of Nanostructured One Dimensional Titanium Dioxide by Synchrotron Radiation and Spectroscopy, Master thesis, The University of Western Ontario, Canada (2013).

[18] R. A. Voloshin, M. V. Rodionova, S. K. Zharmukhamedov, H. J.M. Hou, J. R. Shen and S. I. Allakhverdiev, Applied Photosynthesis - New Progress, Intech Open, (2016), 181.

[19] R. Vidhya, R. Gandhimathi, M. Sankareswari, P. Malliga, J. Jeya and K. Neivasagam, Synthesis and Characterization of Cu Doped TiO_2 Thin Films to Protect Agriculturally Beneficial Rhizobium and Phosphobacteria from UV Light, J Nanostruct, 8(3), (2018), 232-241.

[20] P. Knauth, J. Schoonman, Nanostructured Materials Selected Synthesis Methods, Properties and Applications, United States of America, Kluwer Academic Publishers, (2004), 23.

[21] L. Zhou, L. Wei, Y. Yang, X. Xia, P. Wang, J. Yu, T. Luan, Improved performance of dye sensitized solar cells using Cu-doped TiO2 as photoanode materials: Band edge movement study by spectroelectrochemistry, Chemical Physics, 475, (2016), 1-8.

[22] C.Y .Tsai, H.C. Hsi, T.H. Kuo, Y.M Chang, J.H. Liou, Preparation of Cu-Doped TiO_2 Photocatalyst with Thermal Plasma Torch for Low-Concentration Mercury Removal, Aerosol and Air Quality Research, 13, (2013), 639–648.

[23] H .A. Ahmed, S. I. Abu-Eishah, A. I. Ayesh and S. T. Mahmoud, Synthesis and characterization of Cu-doped TiO_2 thin films produced by the inert gas condensation technique, Journal of Physics, 869, (2017).

[24] P. Tipparak, O. Wiranwetchayan, W. Promnopas, Preparation and characterization of copper doped titanium dioxide thin film by sparking process, SNRU Journal of Science and Technology, 9 (3), (2017), 583-591.

[25] Z. Essalhi, B. Hartiti, A. Lfakir, M .Bernabé, P. Thevenin, Optoelectronics properties of TiO_2: Cu thin films obtained by sol gel method, Opt Quant Electron, 49, 301, (2017).

[26] R. Vidhya, R. Gandhimathi, M. Sankareswari & K. Neyvasagam, Influence of Cu concentration on the structural, morphological, optical and catalytic properties of TiO_2 thin films, Indian Journal of Pure & Applied Physics, 57, (2019), 475-482 .

[27] W. Sangchay, L. Sikong and K. Kooptarnand, The Photocatalytic and Antibacterial Activity of Cu-Doped TiO_2 Thin Films, Walailak J Sci & Tech, 10(1), (2013), 19-27.

[28] A. M. Vathani, S. Dhanalakshmi, N. Prithivikumaran, Synthesis and electrochemical studies on Cu-TiO_2 thin films deposited by spray pyrolysis technique for sensing Uric acid, Int. J. Nano Dimens., 10 (3), (2019), 230-241 .

[29] A. Noua, Preparation and characterization of thin films nanostructures based on ZnO and other oxides, Ph.D thesis, Larbi Ben M'hidi University, Oum El Bouaghi, (2019).

[30] I. Cimieri, Sol-gel preparation and characterization of titanium dioxide films for degradation of organic pollutants, PhD thesis, Ghent University, Belgium (2014).

[31] R. Vidhya, M. Sankarewari, K. Neyvasagam, Effect of Annealing Temperature on Structural and Optical Properties of Cu-TiO_2 Thin Film, International Journal of Technical Research and Applications, 37, (2016), 42-46.

[32] A. Bergauer, C. Eisenmenger-Sittner, "Thin Film Technology/Physics of Thin Films", Vienna, Vienna University of Technology, Austria, 113, (2017).

[33] O. Benkhetta, Effect of the concentration of the solution on the properties of thin films of titanium dioxide deposited by ultrasonic spray pyrolysis, Master thesis, University Mohamed Khider of Biskra, (2019).

[34] R. Zernadji, K. Berramdane, Optimization of Ti/TiO_2 multilayers deposition parameters for corrosion applications, Master thesis, University Mohamed Khider of Biskra, (2019).

[35] A. Mercurio, Impact of TiO_2 electron transport layer properties on planar Perovskite solar cells, Master thesis, Polytechnic University of Catalonia, USA (2017).

[36] M. Tosa, Compendium of Surface and Interface Analysis, Springer, The Surface Science Society of Japan, 679-680, (2019).

[37] V. Rajendran, G. Rajendran, N. Karuppathevar, Phtotocatalytic Degradation of Methyelene Blue by Cu Doped TiO_2 Thin Films under Visible Light Irradiation, Mechanics, Materials Science & Engineering, 2412-5954, (2017).

[38] P. Malliga, J. Pandiarajan, N. Prithivikumaran & K. Neyvasagam , Influence of Film Thickness on Structural and Optical Properties of Sol – Gel Spin Coated TiO_2 Thin Film, IOSR Journal of Applied Physics (IOSR-JAP), 6, Issue 1 ,(2014), 22-28 .

[39] R. Vidhya, M. Sankareswari, P. Malliga, B. Karunai Selvi and K. Neyvasagam, Effect of UV Screening Nature of Cu-TiO_2 Thin Films on the Protection of Chlorophyll Content in Medicinal Plants, J. Nano. Adv. Mat. 5, No. 2, (2017), 75-80.

[40] Ahlam Zekaik, Hadj Benhebal, and Bedhiaf Benrabah, Synthesis and characterization of Cu doped chromium oxide (Cr_2O_3) thin films, High Temp. Mater, 38, (2019), 806–812.

[41] Ibrahim Dundar, Marina Krichevskaya, Atanas Katerski and Ilona Oja Acik, TiO_2 thin films by ultrasonic spray pyrolysis as photocatalytic material for air purification, R. Soc. open sci, 6, (2019).

Abstract

Pure and copper doped titanium dioxide thin films were deposited onto glass substrates by sol-gel dip coating technique. The films were annealed at 400 °C for 3 h and characterized by X-ray diffraction (XRD), scanning electron microscope (SEM) and UV-Visible spectroscopy. The effect of copper doping with different concentrations on the structural, morphological and optical properties of TiO_2 thin films was studied. The XRD results revealed that the Pure and Cu-TiO_2 thin films have anatase phase with preferential orientation along (101) plane. The SEM micrographs show that the surface of the films was loosely agglomerated with cracks and irregular smaller grains. EDX analysis exposes the presence of Ti, O and Cu in the prepared films. The direct and indirect energy band gap of the pure and Cu-TiO_2 thin films was varied between 2.9 and 3.8 eV.

Keywords: thin films, Cu-TiO_2, Dip coating, structural properties, optical properties.

Résumé

Des couches minces de dioxyde de titane pur et dopé au cuivre ont été déposées sur des substrats de verre par la technique sol-gel dip coating. Les couches ont été recuites à 400 °C pendant 3 h et caractérisées par diffraction des rayons X (XRD), microscope électronique à balayage (MEB) et Spectroscopie UV-visible. L'effet du dopage au cuivre à différentes concentrations sur les propriétés structurelles, morphologiques et optiques des couches minces de TiO_2 a été étudié. Les résultats XRD ont révélé que les couches minces pures et dopées (Cu-TiO_2) ont une phase anatase avec une orientation préférentielle le long du plan (101). Les micrographies SEM montrent que la surface des couches était vaguement agglomérée avec des fissures et des grains plus petits et irréguliers. L'analyse par EDX révèle la présence de Ti, O et Cu dans les couches préparées. La bande interdite d'énergie directe et indirecte des couches minces pures et dopées (Cu-TiO_2) a varié entre 2,9 et 3,8 eV.

Mots clés : couches minces, Cu-TiO_2, Dip coating, propriétés structurelles, propriétés optiques.

ملخص :

تم ترسيب الشرائح الرقيقة لثاني أكسيد التيتانيوم النقي و المطعم بالنحاس على مساند زجاجية بتقنية الصول–جل الطلاء بالغمر، و تم تلدين الشرائح عند 400 درجة مئوية لمدة 3 ساعات وتوصيفها بواسطة انعراج الأشعة السينية (XRD) ، المجهر الإلكتروني الماسح (SEM) و مطيافية الأشعة فوق البنفسجية– المرئية. تمت دراسة تأثير التطعيم بالنحاس بتركيزات مختلفة على الخصائص البنيوية، المورفولوجية والضوئية للشرائح الرقيقة لـ TiO_2 . كشفت نتائج XRD أن الشرائح الرقيقة لثاني أكسيد التيتانيوم النقي و المطعم بالنحاس لها طور anatase مع اتجاه تفضيلي على طول المستوى (101). توضح الصور SEM المجهرية أن سطح الشرائح كان متكتلًا بشكل حر مع شقوق وحبيبات صغيرة غير منتظمة. بين تحليل EDX وجود Ti ، O و Cu في الشرائح المحضرة. تراوح نطاق الطاقة المباشر وغير المباشر للشرائح الرقيقة لثاني أكسيد التيتانيوم النقي و المطعم بالنحاس بين 2,9 و 3,8 الكترون فولت.

الكلمات المفتاحية: الشرائح الرقيقة، $Cu–TiO_2$، طلاء بالغمر، الخصائص البنيوية، الخصائص الضوئية.